Chapter 1
Skeletal Muscle Biopsy Evaluation

Dennis K. Burns

Introduction

First introduced into clinical practice in the middle decades of the nineteenth century, muscle biopsies have played an integral role in the diagnosis and treatment of patients with neuromuscular diseases for well over a century. The interpretation of morphological changes in skeletal muscles, supplemented by enzyme histochemical and immunohistochemical stains are now regularly integrated with molecular analyses to provide physicians with an unprecedented understanding of the pathogenesis and phenotypic complexities of neuromuscular diseases. Although advances in molecular diagnoses have eliminated the need for muscle biopsies in some disorders, in many conditions, biopsies continue to provide information not readily obtainable by other methods.

Muscle Biopsy Acquisition

There are three important aspects of muscle biopsy acquisition: selecting the proper muscle, obtaining an adequate amount of tissue, and minimizing artifacts.

The importance of selecting the right muscle for biopsy cannot be overemphasized. Skeletal muscles are not equally affected by a given disease process. While the majority of myopathies predominantly affect proximal limb muscles, a few preferentially involve distal limb, trunk, or facial muscles. In order to maximize the diagnostic yield of a muscle biopsy, it is important to carefully select the biopsy site. Selection of the biopsy site can be challenging and should be done in close consultation with the

D. K. Burns (✉)
Department of Pathology, Neuropathology Section, University of Texas Southwestern Medical Center, Dallas, TX, USA
e-mail: dennis.burns@utsouthwestern.edu

L. Zhou et al. (eds.), *A Case-Based Guide to Neuromuscular Pathology*,
https://doi.org/10.1007/978-3-030-25682-1_1

treating physician. The site of the biopsy should be based on the pattern of muscle weakness, electromyography (EMG) abnormalities, and/or muscle imaging findings [1, 2]. In patients with chronic muscle injury, one should choose a muscle for biopsy that is weak but not profoundly atrophic. If a muscle is markedly atrophic, the biopsy may show "end-stage" changes with extensive fibro-fatty tissue replacement and few residual myofibers, precluding determination of the cause of the muscle injury. In patients with more acute or subacute muscle injury, in contrast, one may choose to biopsy a more severely affected muscle to better capture the muscle pathology. Since the majority of myopathies affect predominantly proximal limb muscles, deltoid, biceps, and quadriceps muscles are most commonly chosen, and these muscles have sufficient norms established for comparing myofiber size and fiber type percentages [3, 4]. If a myopathy predominantly affects distal limb muscles, the tibialis anterior or gastrocnemius muscle may be selected for biopsy. One should not choose a muscle which had recent injection or needle EMG examination, in order to avoid areas of nonspecific muscle injury caused by the needle [5]. Since muscle involvement in myopathies is typically symmetrical, needle EMG of limb muscles is usually done on one side and the biopsy is taken from corresponding contralateral muscle. It is worth mentioning that EMG can be normal in a mild myopathy, and some myopathies may have focal or asymmetrical limb muscle involvement. In these settings, skeletal muscle MRI or ultrasound is sometimes useful in targeting an affected muscle for biopsy.

As discussed in detail in the next few paragraphs, skeletal muscle can be obtained via open biopsy approach [2] or percutaneously, the latter employing a Bergstrom-type cutting needle [1, 6–8]. As an aside, "thin" needles of the type employed in fine needle aspiration biopsies seldom yield adequate material for meaningful interpretation of muscle morphology, and are almost never satisfactory for detailed enzyme histochemical and immunohistochemical studies. For these reason, we recommend that they not be used to obtain muscle biopsies in clinical work. Percutaneous biopsy has the advantage of being less invasive, while open biopsy has the advantage of providing larger specimens [1, 2]. Both procedures are quite safe in the hands of experienced operators. Open biopsy is usually done in an operating room with the patient sedated and under the care of an anesthesiologist, while percutaneous needle biopsies are often performed in outpatient clinic settings. Local anesthesia is given before a skin incision is made, taking care to not infiltrate the muscle tissue selected for biopsy with the anesthetic agent. The incision, typically around 3–4 cm in length, should be made in an area that avoids myotendinous junction whenever possible. Bleeding is usually minimal and can be controlled by firm pressure or ligation without the need for cautery. Muscle biopsy tissue should never be cauterized, inasmuch as the electrocautery destroys muscle morphology and enzyme activity. Detailed muscle biopsy procedures have been described by others [1, 2].

Initial Processing and Sectioning of Skeletal Muscle Biopsies

Procedures for processing skeletal muscle biopsies are well-established and, while not overly complex, differ significantly from procedures employed in handling most tissues submitted to surgical pathology laboratories. If muscle

biopsies are not to be processed in the laboratory that initially receives the specimen, it is essential that the physician obtaining the biopsy and laboratory personnel at the institution where the biopsy is obtained communicate in advance with the laboratory that will ultimately process the specimen to ensure that tissue preservation is optimum.

For optimum evaluation, skeletal muscle biopsies should include both unfixed and fixed tissue. Properly frozen, unfixed tissue, in particular, plays a critical role in the assessment of morphological abnormalities in skeletal muscle. Fresh muscle should be transported immediately to the laboratory for freezing and subsequent processing. During transportation to the laboratory, the fresh tissue should be wrapped in gauze that has been slightly moistened in saline and placed in a waterproof container surrounded by crushed wet ice, in order to prevent drying artifact and loss of enzyme activity. The amount of saline should be sufficient to simply keep the tissue moist; excess saline can introduce freezing artifact, as well as promote a loss of enzyme activity in the muscle. Ideally, muscle biopsies should be transported to the laboratory for freezing within 60 minutes of the procedure, although satisfactory morphology can be obtained in tissue frozen within a few hours of the biopsy, as long as the specimen is kept cool. For specimens being transported overnight, it is advisable to freeze the specimen in the referring laboratory, and then transport the specimen on dry ice to the reference laboratory for processing.

As soon as the specimen arrives in the laboratory, the muscle segment should be carefully oriented so that its fibers are in cross section. In the case of larger segments, orientation can often be accomplished with the naked eye, while smaller specimens, including those obtained via a percutaneous needle biopsy, are best oriented with the aid of a dissecting microscope (Fig. 1.1a). The oriented sample is placed on an appropriately-labeled cork segment and immobilized with a small amount of either gum tragacanth or a small amount of Optimal Cutting Temperature (OCT) mounting medium at the base of the tissue. It is important that the tissue be placed *on top of the mounting medium* rather than covered by the medium, so that subsequent freezing of the tissue can occur as rapidly as possible (Fig. 1.1b).

Once oriented and immobilized on the cork, the fresh muscle is ready for freezing. The basic tools for freezing are relatively simple, and include a suspended metal beaker, an insulated container for liquid nitrogen and a supply of isopentane (Fig. 1.2a). The oriented skeletal muscle segment is frozen by placing it into a metal beaker of isopentane that has been cooled in liquid nitrogen to approximately −160° C. The isopentane will be sufficiently chilled when a delicate white rind begins to form on the inner surface of the beaker. The specimen should be completely immersed and gently stirred in the chilled isopentane in order to facilitate rapid, uniform freezing of the tissue (Fig. 1.2b). For smaller specimens, freezing is usually complete within 30 seconds, while larger specimens may require immersion for up to 50 seconds. Once the tissue has been frozen, it can be transferred directly to the cryostat for sectioning or, alternatively, stored in a sealed plastic bag at −70 to −80 °C. If long term storage is anticipated, placing a few ice crystals into the plastic bag can minimize “freezer burn” during storage.

In order to prepare frozen sections, the cork holding the specimen should be immobilized on a standard cryostat chuck using OCT embedding medium.

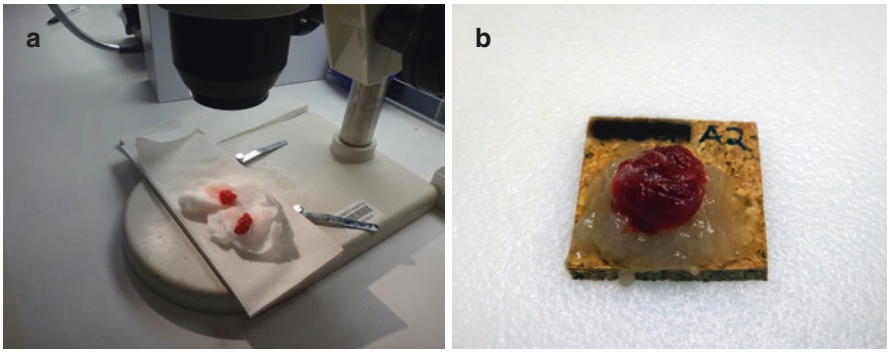

Fig. 1.1 Orientation of the muscle biopsy. (**a**) Larger specimens can sometimes be oriented with the naked eye, but in many cases, the use of a dissecting microscope can ensure that cross sections of the fresh frozen specimen are obtained. (**b**) A properly oriented muscle segment. The fresh tissue has been mounted on the surface of a small mound of gum tragacanth. Note that the specimen is not fully embedded in the mounting medium. This ensures that a maximum amount of the specimen's surface area is exposed to the chilled isopentane (2-methlybutane) during the subsequent freezing process

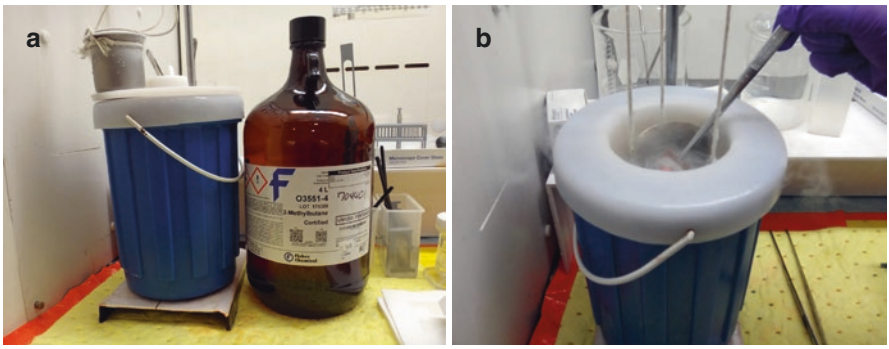

Fig. 1.2 Freezing the muscle biopsy. (**a**) The basic material for properly freezing muscle biopsies consists of an insulated, wide-mouthed container for liquid nitrogen, a metal beaker that can be suspended into the liquid nitrogen and a supply of isopentane. (**b**) To freeze the biopsy, the metal beaker is filled with isopentane and partially immersed into the liquid nitrogen, taking care to not allow the liquid nitrogen to come into direct contact with the isopentane. A white rind will form on the inner surface of the metal beaker when the isopentane has been cooled to an appropriate temperature for freezing the specimen. The oriented, mounted muscle segment is then completely immersed in the chilled isopentane and gently stirred for about 50 seconds. Once frozen, the specimen can be transferred to the cryostat for sectioning or, alternatively, stored in a sealed plastic bag at −70 to −80° C for later processing

Sections should be cut in a cryostat maintained at a temperature of −20 to −25° C. Biopsies that have been stored at −70 to −80 °C should be allowed to warm to cryostat temperatures in order to avoid shattering the tissue during sectioning. Sections of tissue destined for routine staining, including enzyme histochemical staining, should be cut at thicknesses of 10 μm, while those used for immunohistochemical staining should be cut a thicknesses of 6 μm. In our laboratory, sections are picked up directly onto commercially prepared posi-

tively-charged glass slides (*Superfrost™ Plus*), although sections can also be placed on standard glass coverslips for staining if desired. If the cryostat sections are not to be stained immediately, the slides are placed in a folder and kept in a 4 °C refrigerator until ready for use. Ideally, cryostat muscle sections should be stained within 24 hours of the time that the sections are cut.

Although skeletal muscle morphology at the light microscopic level is best demonstrated in cryostat sections of properly frozen muscle, fixed muscle can also provide useful diagnostic information in a number of important muscle disorders. In the case of open biopsies, muscle destined for fixation should be clamped *in situ* using either a single use, disposable Becton Dickinson Rayport® polypropylene clamp or a reusable Price muscle biopsy clamp. The clamped muscle segment is gently excised from the surrounding skeletal muscle, placed into 10% neutral buffered formalin, and transported to the laboratory. Once in the laboratory, the fixed muscle segment is excised from the clamp. Representative longitudinally oriented sections measuring no more than 1 mm in thickness are transferred to 3% buffered glutaraldehyde for resin embedding and, in selected cases, subsequent electron microscopy. The remainder of the skeletal muscle segment is divided into cross and longitudinal sections and placed into standard histological cassettes for paraffin histology, discussed below. Muscle tissue obtained via percutaneous needle biopsy is also suitable for fixation. Muscle fragments obtained via needle biopsy can be placed directly into fixative—either 10% neutral buffered formalin or 3% buffered glutaraldehyde—and transported to the laboratory.

Routine Histological Stains

Proper evaluation of muscle biopsies requires the use of a number of different stains on frozen and, in some laboratories, fixed tissue, some of which are familiar to general surgical pathologists and some of which are used exclusively in the evaluation of frozen skeletal muscle. In our laboratory, frozen and paraffin sections of skeletal muscle biopsies are routinely evaluated with a panel of non-enzymatic histological stains and enzyme histochemical stains as listed below:

- Non-enzymatic stains (frozen sections)
  - Hematoxylin and eosin (H&E)
  - Modified Gomori trichrome
  - Oil Red O
  - Non-aqueous periodic acid Schiff (PAS) with and without diastase digestion (usually reserved for cases with suspected glycogen storage abnormalities)
  - Crystal violet
  - Congo red
- Enzyme histochemical stains (frozen sections)
  - Myosin adenosine triphosphatases (ATPases) at pH 4.3, 4.6 and 9.4
  - Nonspecific esterase
  - Acid phosphatase

  - Alkaline phosphatase
  - NADH-tetrazolium reductase
  - Succinate dehydrogenase (SDH)
  - Cytochrome-c oxidase (COX)
  - Sequential COX-SDH
  - Myophosphorylase
  - Phosphofructokinase
  - Myoadenylate deaminase
- Non-enzymatic stains (paraffin sections)
  - H&E
  - Masson trichrome
  - Congo red
  - Morin stain (reserved for cases of suspected aluminum adjuvant-associated myopathies)

Most of the staining of frozen (cryostat) sections is performed by placing the mounted sections in new 5-slide capacity plastic slide mailers. Coplin jars are used for the same purpose in some institutions, but if used, must be scrupulously cleaned between staining runs to avoid cross contamination. The use of new slide mailers minimizes the risk of such cross contamination. Individual stains and their uses are described in the following paragraphs. Technical information about individual staining procedures is available in published protocols included in the references at the end of this chapter [1, 9–18].

Normal skeletal muscle is composed of a mixture of three different types muscle cells, each of which has a fairly predictable staining profile in the panel of stains listed above. Type 1 myofibers, also known as "slow twitch" fibers, generate most of their energy via oxidative metabolism, and, as such, have abundant mitochondria and lipid, and less glycogen. Type 1 fibers are relatively resistant to fatigue, and are adapted to prolonged, endurance-type activities. Type 2 myofibers, or "fast twitch" fibers, generate more of their energy via glycolysis and contain more abundant glycogen and have less lipid and fewer mitochondria than their type I counterparts. Type 2 myofibers can be further subdivided into type 2a (fast twitch mixed oxidative/glycolytic) fibers and type 2b (fast twitch glycolytic) fibers. Type 2a fibers can change into type 2b fibers and vice versa, depending upon an individual's exercise habits. Whether of myofiber is a type 1 or a type 2 fiber, however, is determined by the lower motor neuron that innervates it and remains constant if its innervation remains intact. The metabolic profile of a given myofiber influences its staining properties, as discussed in the following paragraphs.

Non-enzymatic Stains (Frozen Sections)

The ***hematoxylin and eosin (H&E) stain*** is arguably the single most useful stain used in the evaluation of frozen sections of skeletal muscle biopsies. H&E stained cryostat sections provide information about the presence and pattern of myofiber

atrophy (e.g., group atrophy in neurogenic disorders, selective perifascicular atrophy in classical dermatomyositis), myofiber degeneration and necrosis, regenerative change, vacuoles, inflammatory infiltrates and chronic structural changes of the type seen in many muscular dystrophies. Blood vessels and structural vascular abnormalities (e.g. vasculitis) are also well demonstrated in H&E sections. In normal muscle (Fig. 1.3a), individual myofibers have a polygonal configuration in cross section, with diameters ranging from approximately 30–70 mμ in adult women and 40–80 mμ in adult men [19]. Myofiber nuclei stain blue in H&E sections. Normal myofiber nuclei are small, and typically lie at the periphery of the fiber in transverse sections. Contractile proteins give the sarcoplasm a light pink appearance. Delicate basophilic stippling is visible in well preserved specimens at higher magnification, imparted by the presence of mitochondria and "sarcotubular" components (sarcoplasmic reticulum and T-tubules) in the intermyofibrillar network. Type 1 myofibers stain a bit more darkly than type 2 fibers in H&E stains, although fiber typing is best done with other stains (see below). When muscle fibers regenerate following myofiber injury, the sarcoplasm often stains light blue, owing to the presence increased cytoplasmic ribonucleoprotein associated with protein synthesis. Enlarged nuclei with discernible nucleoli are another characteristic of regenerating myofibers. These changes are illustrated later under the heading "Interpretation of the Biopsy." Increased numbers of internalized nuclei can be seen in a number of myopathic disorders (discussed below) but are also common near myotendinous insertion sites, and in this location should not be interpreted as evidence of myofiber injury.

The ***Gomori trichrome stain*** is familiar to most pathologists as a useful stain for demonstrating collagen, which stains with a light green color in frozen sections. In frozen sections of skeletal muscle, the modified Gomori trichrome stain developed by Engel and Cunningham [9] plays an even more important role in highlighting a variety of normal and abnormal structures within the sarcoplasm of muscle fibers. Normal mitochondria and sarcotubular elements, which are visible as punctate blue structures in H&E sections, stain red in the Gomori trichrome stain owing to the affinity of sarcoplasmic membranous structures for the Chromotrope 2R dye used in the procedure (Fig. 1.3b). Abnormal collections of mitochondria produce characteristic "ragged red" change in type I myofibers in many patients with mitochondrial disorders (discussed below under "Interpretation of the Biopsy"). Tubular aggregates, discussed below in the paragraphs dealing with biopsy interpretation, are also highlighted in the Gomori trichrome stain. Additional structures that are reliably highlighted in the trichrome stain include nemaline rods and cytoplasmic bodies (both derived from sarcomeric Z-bands), and the membranous debris present in sarcoplasmic vacuoles in patients with inclusion body myositis. Figures 1.18–1.20, which will be discussed later, contain examples of some of the abnormal structures that are highlighted in Gomori trichrome-stained cryostat sections. The appearance of collagen in Gomori trichrome-stained cryostat sections is illustrated in Fig. 1.21, which will also be discussed later.

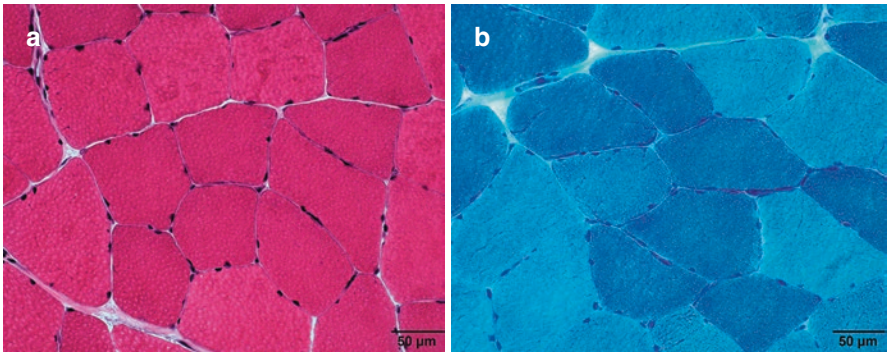

Fig. 1.3 Normal muscle (H&E and Gomori trichrome stains) **.** (**a**) Normal skeletal muscle, H&E. In a properly prepared skeletal muscle segment, the myofibers have a fairly uniform, polygonal appearance in cross section. The sarcoplasm of normal muscle fibers stains pink H&E stains, due to the presence of contractile proteins (myofibrils). In normal muscle myofiber nuclei characteristically lie just beneath the sarcoplasm except in the vicinity of myotendinous insertion sites, where internalized nuclei are fairly common. (**b**) Normal skeletal muscle, Gomori trichrome. The Gomori trichrome stain is an indispensable stain in the evaluation of frozen muscle biopsies. The contractile proteins stain green in the Gomori trichrome stain, while the membrane-rich elements that lie between the myofibrils (mitochondria, sarcoplasmic reticulum and T-tubules) stain red-purple, imparting a delicate stippled appearance to the sarcoplasm. Type 1 myofibers have larger numbers of mitochondria than type 2 fibers and stain more darkly in the Gomori trichrome stain

The ***Oil Red O stain*** is one of several stains available for demonstrating sarcoplasmic neutral lipid in frozen sections. Neutral lipid is present in normal skeletal muscle, particularly in type I (slow twitch) fibers. Normal sarcoplasmic lipid appears as fine red dots in the Oil Red O stain (Fig. 1.4a), and abnormal lipid stores appear as correspondingly larger red droplets (Fig. 1.4b). "Bleeding" of stained lipid over the section can occur when the muscle biopsy contains a significant amount of adipose tissue, and care must be taken to not misinterpret this phenomenon as abnormal sarcoplasmic lipid accumulation. After staining, sections are covered with glycerol or a comparable aqueous medium and coverslipped.

Periodic Acid-Schiff (PAS) stains have been used for decades to demonstrate carbohydrates in tissues, including glycogen and other molecules with carbohydrate components (e.g., glycoproteins and glycolipids). PAS stains are especially important in the evaluation of biopsies from patients with suspected glycogen storage diseases. Carbohydrate-rich structures, including glycogen, stain magenta in the PAS stain (Fig. 1.4c, d). Incubation of the tissue with diastase before staining will remove particulate glycogen, but will leave other carbohydrate-bearing structures (e.g. basement membranes) intact. The PAS reactivity basement membranes and of abnormal filamentous forms of glycogen of the type that accumulate in type IV glycogenosis and polyglucosan body disease is not affected by diastase digestion. It is worth noting that fixation of tissue in aqueous fixatives prior to staining often removes delicate particulate glycogen from the tissues, preventing adequate demonstration of abnormal glycogen stores.

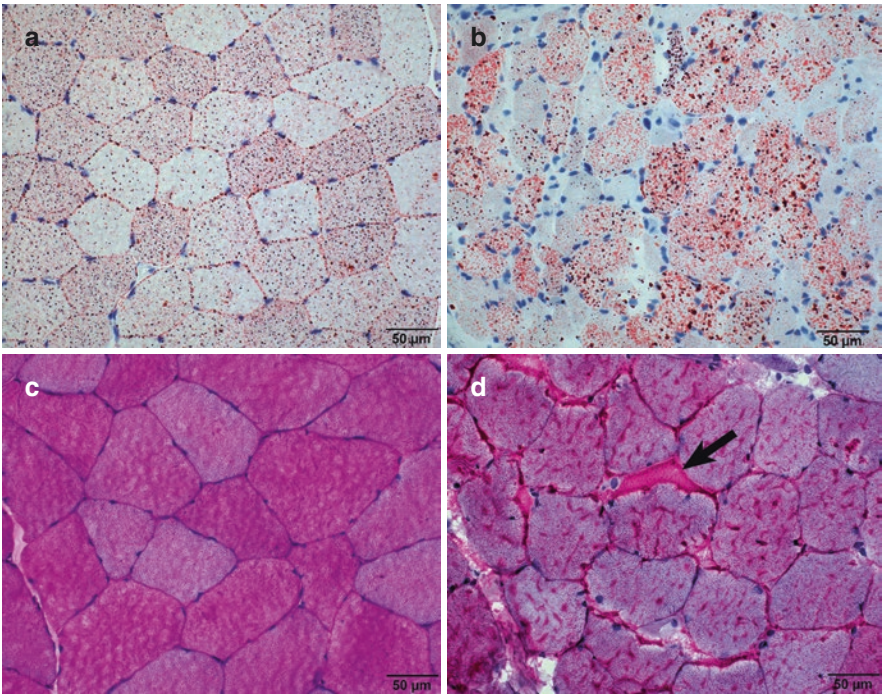

Fig. 1.4 Oil red O and PAS-stains of frozen muscle. (**a**) Normal muscle, oil red O. The oil red O stain is a very useful stain for demonstrating neutral lipids in frozen muscle, which appear as delicate red sarcoplasmic droplets. The lipid content of type 1 myofibers is higher than that of type 2 fibers. (**b**) Lipid storage myopathy, oil red O. Abnormal sarcoplasmic lipid accumulation can be seen in a wide range of conditions, including primary lipid storage myopathies, as illustrated here. Increased amounts of lipid are also seen in mitochondrial disorders and as a nonspecific reaction to myofiber injury. The abnormal lipid deposits appear as larger droplets than those seen in normal muscle. In extreme cases, these large droplets can occupy most of the cross sectional area of the affected myofiber. (**c**) Normal muscle, PAS. The PAS stain is the standard stain for demonstrating glycogen and basement membrane material. Because type 2 myofibers have a higher concentration of glycogen than type 1 fibers, they stain more intensely in the PAS stain. Incubation of the tissue section with diastase (amylase) will remove particulate glycogen, but will not affect the staining of basement membranes. (**d**) Glycogen storage disease, PAS. Abnormal glycogen deposits (arrow) stain with a magenta color in the PAS stain. In this biopsy from a patient with McArdle disease (muscle phosphorylase deficiency), particulate glycogen accumulates in subsarcolemmal regions. Pre-treatment with diastase will remove such deposits. In some conditions, exemplified by glycogen storage disease type IV and polyglucosan body disease, the abnormal glycogen deposits are composed of filamentous rather than particulate glycogen and will persist in the tissue after diastase digestion

The ***Congo Red stain*** is an essential stain for demonstrating amyloid deposits. The term "amyloid" does not refer to a specific protein, but rather to a heterogeneous group of proteins that have in common a tendency to aggregate into a β-pleated sheet configuration. Amyloid deposits can be encountered in skeletal muscle in patients with sporadic systemic amyloidosis, most commonly associated with plasma cell dyscrasias and abnormal immunoglobulin light chain (particularly lambda light chain) production. Less commonly, amyloid deposits can be seen in hereditary forms of amyloidosis associated with abnormal deposits of transthyretin and, less commonly, a

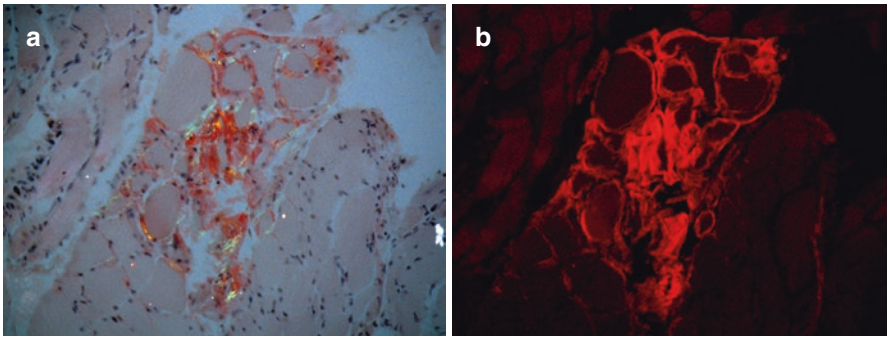

Fig. 1.5 Amyloid deposits, Congo red stain. (**a**) Amyloidosis, Congo red under polarized light. The classic method for the demonstration of amyloid deposits at the light microscopic level is the Congo red stain. When viewed under polarized light, the pink-staining amyloid has a characteristic "apple green" birefringence. (**b**) Amyloidosis, Congo red with epifluorescence illumination. When Congo red-stained sections are viewed under epifluorescence illumination with Texas red filtration, amyloid deposits have a bright red appearance. This technique is a more sensitive method for detecting amyloid deposits than polarized light microscopy, but is somewhat less specific

number of other proteins. Interestingly, amyloid deposition is also seen in two forms of autosomal recessive limb girdle muscular dystrophy – LGMD 2B (dysferlinopathy) [20] and LGMD 2 L (anoctamin-5 deficiency) [21]. In all of the preceding conditions, the amyloid is deposited extracellularly – most commonly within vessels walls and around individual myofibers. Intracellular amyloid deposits also occur in some conditions, notably variants of inclusion body myositis (IBM). In this disorder, the intracellular amyloid deposits are composed of β-amyloid, the type of amyloid encountered in the central nervous system in Alzheimer's disease and amyloid angiopathy.

Amyloid deposits appear as homogeneous, eosinophilic deposits in in H&E stained sections, and have a salmon-pink color in Congo red stains. Under polarized light, the amyloid deposits contain areas of characteristic "apple green" birefringence (Fig. 1.5a). Fluorescence microscopy with Texas Red filtration is an even more sensitive technique for detection of amyloid deposits [22]. Under fluorescence illumination with Texas Red filtration, amyloid deposits appear bright red (Fig. 1.5b).

Enzyme Histochemical Stains (Frozen Sections)

Staining for ***myosin adenosine triphosphatase (ATPase)*** activity has long been the most reliable method for distinguishing slow twitch (type 1) myofibers from fast twitch (type 2) fibers. The staining procedure involves the cleavage of a phosphate group from ATP in a frozen muscle section in a solution of aqueous calcium chloride, producing an insoluble calcium phosphate precipitate at the site of the reaction. The tissue is then incubated in a solution of cobaltous chloride, during which the calcium in the calcium phosphate is replaced by cobalt (Co^{2+}). The section is then briefly incubated in a solution of ammonium sulfide, which generates a black cobaltous sulfide reaction product in the muscle fiber [1, 10, 11]. Incubation of the section in an alkaline barbital solution (pH 9.4 in our laboratory) results in the selective

activation of myosin ATPase in type 2 fibers, causing them to stain darkly, while type 1 fibers remain pale. Pre-incubation of tissue sections in a barbital buffer at pH 4.3 produces a reciprocal staining pattern – that is, darkly staining type 1 fibers and pale type 2 fibers. In addition, in the ATPase 4.3 preparation, a small subpopulation of intermediate-staining type 2c fibers is often visible. Finally, pre-incubation of the tissue section at pH 4.6 produces a pattern in which type 1 fibers stain darkly, type 2a (fast twitch oxidative) fibers are pale, and type 2b (fast twitch glycolytic) fibers stain with intermediate intensity (Fig. 1.6a–c). The use of standard mounting medium in the preparation of slides stained for ATPase activity will result in fading of the reaction product over time. Staining intensity can be preserved by coverslipping the ATPase-stained sections with Canada balsam. In normally innervated muscle, the distribution of type 1 and type 2 fibers is random, as illustrated in Fig. 1.6a–c. A loss of randomness in the distribution of myofibers is called "fiber

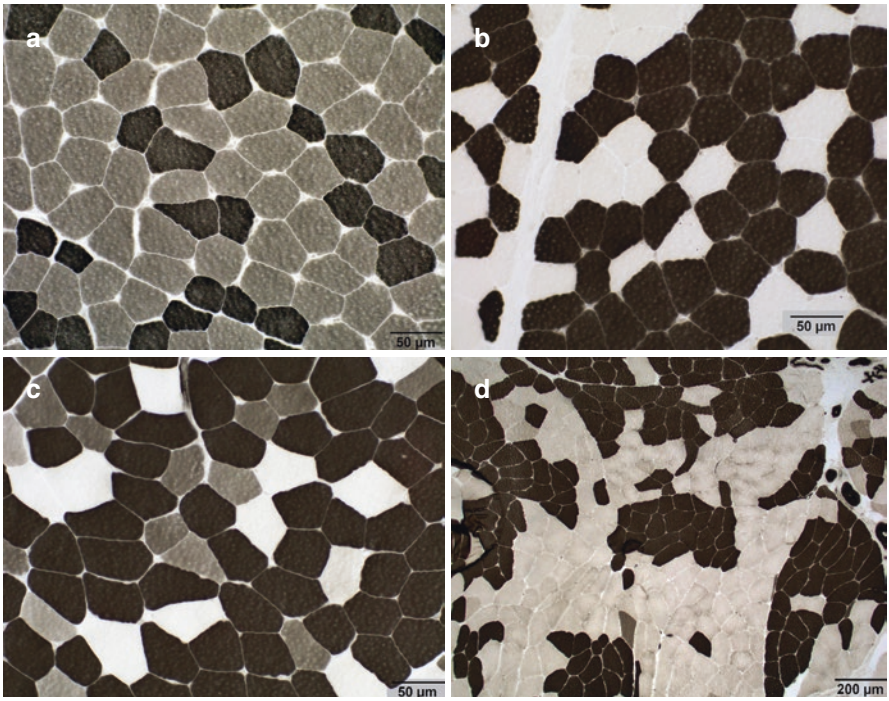

Fig. 1.6 ATPase stains. (**a**) Normal muscle, ATPase 9.4. Cryostat sections stained for myosin ATPase activity are the most reliable way to distinguish slow-twitch (type 1) from fast-twitch (type 2) subpopulations. In this section of deltoid muscle stained for ATPase activity at pH 9.4, type 2 fibers are dark, while type 1 fibers are pale. (**b**) Normal muscle, ATPase 4.3. Staining a section of the same muscle for ATPase activity at pH 4.3 reveals a reverse staining pattern, with the more numerous type 1 fibers staining darkly. (**c**) Normal muscle, ATPase 4.6. Staining of normal skeletal muscle at pH 4.6 typically reveals three levels of staining intensity: type 1 fibers are dark, type 2A (mixed oxidative-glycolytic) fibers are pale, and type 2B (fast twitch glycolytic) fibers stain with intermediate intensity. (**d**) In normal skeletal muscle, the different myofiber subtypes intermingle in a random distribution. If a muscle is denervated and then re-innervated, axonal sprouts from regenerating motor axons innervate contiguous myofibers, resulting in the formation of groups of contiguous myofibers with the same histochemical staining profile ("fiber type grouping")

type grouping" and indicates reinnervation of previously denervated muscle (Fig. 1.6d). The ATPase stain is extremely helpful in characterizing conditions associated with various patterns of type-specific myofiber atrophy or hypertrophy, and in the identification of patients with myopathy with thick filament loss ("critical illness") myopathy. Some of these patterns are illustrated later under "Interpretation of the Biopsy" in Fig. 1.12.

The ***nonspecific esterase stain*** relies on the hydrolysis of an exogenous alpha-naphthyl acetate substrate by endogenous esterase to yield naphthol, which in turn forms an insoluble azo dye when incubated with basic fuchsin, which appears brick red under the microscope [12]. The stain highlights normal neuromuscular junctions due to the presence of acetylcholinesterase in those structures, providing a reliable internal control (Fig. 1.7a). Recently denervated myofibers are highlighted in the esterase stain, owing to increased cytoplasmic esterase activity (Fig. 1.7b). The esterase stain also highlights macrophages and, in some cases, sarcoplasmic vacuoles associated with abnormal lysosomal activity, although these are usually demonstrated even more clearly in sections stained for acid phosphatase activity (discussed below). Type 1 fibers generally stain a bit more darkly than type 2 fibers in the esterase stain.

The ***acid phosphatase stain*** is based on the hydrolysis of naphthol AS-B1 phosphate by endogenous acid phosphatase to form naphthol, which, like the naphthol generated in the esterase stain, forms an insoluble azo dye in the presence of basic fuchsin [1, 11]. The red reaction product highlights macrophages (Fig. 1.7c) and other structures that have lysosomal activity, such as degenerating myofibers and pathological sarcoplasmic inclusions associated with abnormal lysosomal activity (Fig. 1.7d). The stain is generally a more sensitive marker of lysosomal activity than the nonspecific esterase stain.

The ***alkaline phosphatase stain*** is another "hydrolytic" stain that relies on the hydrolysis of an alpha-naphthyl acid phosphate substrate by endogenous alkaline phosphatase to generate naphthol, which reacts, in turn, with a diazo salt (fast blue RR salt) to form a black reaction product at sites of alkaline phosphatase activity. Glycerol or a comparable aqueous mounting medium should be used to coverslip the section, as alcohols or xylene dissolve the reaction product [13]. The alkaline phosphatase reaction generates gas that can produce distracting bubbles if the section is coverslipped prematurely. To minimize this, it is advisable to wait at least 45 minutes before placing the coverslip over the stained section. The stain highlights the sarcoplasm of regenerating myofibers (Fig. 1.7e), as well as occasional myofibers in infantile denervation of the type seen in spinal muscular atrophy type 1 (Werdnig-Hoffmann disease); normal muscle fibers lack alkaline phosphatase activity. Increased alkaline phosphatase reactivity can also be seen in connective tissue in many inflammatory disorders of skeletal muscle. Increased perimysial connective tissue reactivity, in particular, is a feature of some inflammatory myopathies associated with the presence of circulating anti-Jo1 or other anti-tRNA synthetase antibodies (Fig. 1.7f).

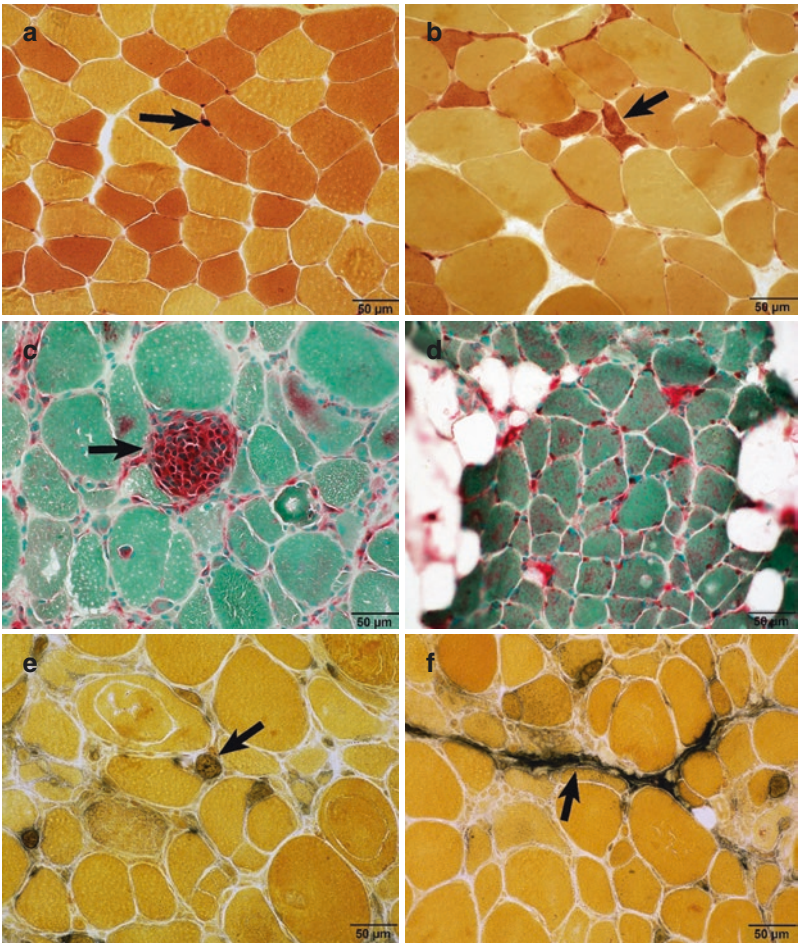

Fig. 1.7 Hydrolytic stains – esterase, acid phosphatase and alkaline phosphatase stains. (**a**) Normal skeletal muscle, esterase. The esterase stain highlight normal neuromuscular junctions (arrow). The brick-red reaction product in these structures is caused by the presence of the enzyme acetylcholinesterase, and serves as a reliable internal control for the esterase stain. (**b**) Denervation atrophy, esterase. The esterase stain is also an effective way to identify atrophic denervated myofibers (arrow), which stain with the same brick-red appearance as normal neuromuscular junctions. (**c**) Myophagocytosis, acid phosphatase. The acid phosphatase stain produces a bright red reaction product in areas of increased enzyme activity, and serves as a reliable marker for lysosomal activity. Activated macrophages contain numerous lysosomes and are highlighted in the acid phosphatase stain, as in the case of these macrophages engulfing the sarcoplasm of a necrotic muscle fiber (arrow). (**d**) Hydroxychloroquine myopathy, acid phosphatase. Abnormal lysosomal activity is a feature of some toxic myopathies. The excessive lysosomal activity in this muscle from a patient with hydroxychloroquine myopathy is responsible for the increased acid phosphatase reactivity in the sarcoplasm of many of these myofibers. (**e**) Myofiber regeneration, alkaline phosphatase. The alkaline phosphatase stain produces a dense black reaction product. This figure highlights areas of abnormal alkaline phosphatase reactivity associated with myofiber regeneration (arrow). (**f**) Inflammatory myopathy, alkaline phosphatase. Abnormal perimysial connective tissue reactivity (arrow) is a feature of inflammatory myopathies associated with the presence of anti-Jo1 and other anti-synthetase antibodies

The ***nicotinamide adenine dinucleotide-tetrazolium reductase (NADH-TR) stain*** is an extremely useful member of the "oxidative" family of stains. The NADH-TR enzyme is a flavoprotein involved in electron transfer in the normal respiratory chain. Both mitochondrial and cytosolic forms of NADH-TR are present in human skeletal muscle, the latter associated with sarcoplasmic reticulum. The NADH-TR staining reaction is based upon the enzymatic removal of hydrogen from exogenous NADH substrate, and the transfer of that hydrogen to nitro blue tetrazolium. The transfer of hydrogen to nitro blue tetrazolium, in turn, generates an insoluble dark blue reaction product, which marks the site of enzyme activity. Sections are coverslipped with an aqueous mounting medium [1, 11, 14]. Mitochondria have NADH-TR activity, and for this reason normal type 1 fibers stain more darkly than type 2 fibers. In optimally stained specimens, some differences in the staining intensity of type 2a versus type 2b fibers may be apparent, with type 2a fibers staining a bit more darkly than type 2b fibers, but this distinction is much more reliably made in the ATPase 4.6 stain, The NADH-TR stain is useful for demonstrating architectural abnormalities within muscle fibers, such as target/targetoid change, sarcoplasmic cores, moth-eaten fibers, sarcoplasmic "whorling", ring fibers and lobulated fibers (discussed later). Denervated myofibers are also variably highlighted in the NADH-TR stain. Abnormal mitochondrial aggregates are sometimes highlighted in the NADH-TR stain, although these are more reliably detected in the succinate dehydrogenase and/or cytochrome c oxidase stains, discussed below. The stain is also useful for the identification of tubular aggregates, structures that are derived from sarcoplasmic reticulum and are sometimes confused with ragged red change in Gomori trichrome-stained sections. An example of a normal NADH-TR stain is illustrated in Fig. 1.8a, and examples of abnormalities highlighted in the NADH-TR stain are illustrated later, under the heading "Interpretation of the Muscle Biopsy."

The ***succinate dehydrogenase (SDH) stain*** identifies a flavoprotein enzyme that is complex II in the mitochondrial respiratory chain. The enzyme is anchored to the inner mitochondrial membrane and is encoded exclusively by nuclear – as opposed to mitochondrial – DNA. SDH normally catalyzes the conversion of succinate to fumarate and the closely linked transfer of electrons to ubiquinone to form ubiquinol in the mitochondrial electron transport chain. In vitro, the SDH stain relies on the ability of SDH to release hydrogen from its sodium succinate substrate and reduce aqueous nitro blue tetrazolium to form a blue tetrazolium precipitate. The stained sections are coverslipped using an aqueous mounting medium [1, 11, 14, 15] The SDH stain is a specific stain for mitochondria, and a much more sensitive marker for mitochondrial aggregation than either the Gomori trichrome stain or the NADH-TR stain. Myofibers harboring abnormal mitochondrial aggregates appear as "ragged blue" fibers in the SDH stain. A normal SDH stain and an SDH stain in a patient with abnormal mitochondrial accumulation are illustrated in Fig. 1.8b, c.

The enzyme ***cytochrome c oxidase (COX)*** is complex IV in the mitochondrial respiratory chain. The enzyme is composed of multiple subunits, three of which are encoded by mitochondrial DNA in mammalian tissue. The COX complex is located in the inner mitochondrial membrane, where it transfers electrons from the cytochrome c

protein to molecules of dioxygen to form water. The COX stain is based on the ability of the enzyme to transfer electrons from an artificial diaminobenzidine tetra hydrochloride substrate to produce an insoluble brown diaminobenzidine precipitate (Fig. 1.8d). Stained sections are coverslipped using an organic mounting medium [1, 11, 14, 15]. Like SDH, COX is a specific marker for mitochondria. Its usefulness in diagnostic work is based on the fact that many mitochondrial disorders are associated with COX deficiency, characterized by failure of affected myofibers to stain in the COX preparation (Fig. 1.8e). In most mitochondrial disorders associated with COX deficiency, SDH reactivity is preserved, and staining sections sequentially for COX and then SDH activities [15] makes detection of COX-deficient fibers a bit easier, with COX-deficient fibers standing out as blue fibers surrounded by brown-staining fibers with intact COX activity (Fig. 1.8f). COX-deficient fibers are common in a number of conditions including primary mitochondrial disorders, including inclusion body myositis and polymyositis with mitochondrial abnormalities [23]. COX deficient myofibers are also seen in some cases of dermatomyositis, wherein there is a selective loss COX activity in perifascicular myofibers [23, 24]. COX is a fairly unstable enzyme, and care must be taken to distinguish artifactual loss of COX activity associated with improper handling of muscle tissue from true COX deficiency; this staining pattern is illustrated later in Fig. 1.24c, under the discussion of Artifacts in Skeletal Muscle Biopsies.

Two standard enzyme histochemical procedures are available for the detection of enzymes associated with glycogen metabolism – muscle-specific phosphorylase (myophosphorylase) and phosphofructokinase. ***Myophosphorylase*** is an enzyme that catalyzes the conversion of glycosyl residues in glycogen to glucose-1-phosphate, which is then used in the generation of ATP. Detection of myophosphorylase is based on the ability of the enzyme to add glucose residues to a glycogen primer in the presence of a large amount of glucose-1-phosphate substrate (the reverse of the reaction sequence that occurs *in vivo*). The resultant glycogen is then stained with Lugol's iodine solution, resulting in a gray-brown reaction product. Sections are coverslipped using an aqueous mounting medium [11, 16]. Patients with myophosphorylase deficiency (type V glycogen storage disease, also known as McArdle's disease) classically present with histories of cramps, exercise intolerance and episodes of rhabdomyolysis following vigorous exercise. In muscle biopsies from such patients, no phosphorylase reaction product is detectable in intact muscle fibers, which appear yellow under the microscope. Myophosphorylase is a labile enzyme that is subject to artifactual degradation, and it is important to distinguish such artifactual losses of enzyme activity from true phosphorylase deficiency. Smooth muscle cells in intramuscular blood vessels express a different isoform of phosphorylase than skeletal muscle, and the identification of residual phosphorylase activity in blood vessel walls serves as an internal control that distinguishes artifactual loss of enzyme activity from selective myophosphorylase deficiency. Of note, the reaction product in the myophosphorylase stain will fade over time, and it is helpful to make a notation of a "positive" result on the slide label. The color of the reaction product can be restored by re-incubating the section in Lugol's solution.

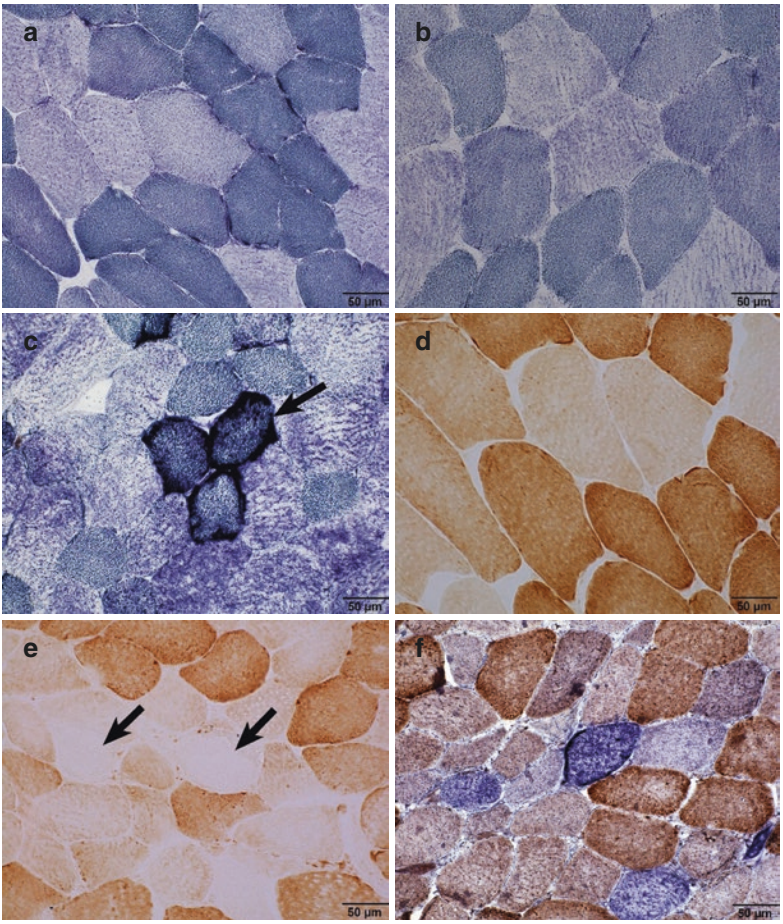

Fig. 1.8 Oxidative stains – NADH-TR, succinate dehydrogenase (SDH) and cytochrome c oxidase (COX). (**a**) Normal muscle, NADH-TR. The NADH-TR stain is highlights both mitochondria and sarcoplasmic reticulum. It is a useful stain for highlighting a wide range of structural sarcoplasmic abnormalities. In normal muscle, as illustrated here, type 1 fibers stain more intensely than type 2 fibers. (**b**) Normal muscle, SDH. The SDH stain has the same reaction product as the NADH-TR stain, and appears very similar to the NADH-TR stain in normal muscle. Unlike the NADH-TR stain, the SDH stain only highlights mitochondria, and is a more sensitive stain for highlighting abnormal mitochondrial aggregates. Owing to their greater numbers of mitochondria, type 1 fibers stain more intensely than type 2 fibers. (**c**) Mitochondrial myopathy, SDH. Abnormal mitochondrial accumulation is associated with intense blue sarcoplasmic reactivity in the SDH stain (arrow). (**d**) Normal muscle, cytochrome c oxidase (COX). The COX stain is another stain that highlights only mitochondria, in this case with a brown reaction product. In normal muscle, the pattern of COX reactivity parallels that of SDH reactivity, with type 1 fibers staining more intensely than type 2 fibers. (**e**) Mitochondrial myopathy, COX. Many mitochondrial myopathies are characterized by abnormalities in COX activity (complex IV in the mitochondrial respiratory chain). Affected muscle fibers in such cases fail to react when stained for COX reactivity (arrows). (**f**) Mitochondrial myopathy, sequential stain for COX and SDH. The sequential COX-SDH stain increases the sensitivity of detection of COX-deficient myofibers. In patients with mitochondrial myopathies associated with COX deficiency, the myofibers that fail to stain for COX activity do not precipitate a reaction product, and retain enzyme activity. If subsequently stained for SDH reactivity, the COX-deficient myofibers stand out as blue-staining fibers surrounded by brown, COX-reactive fibers

Phosphofructokinase (PFK) is a glycolytic pathway enzyme that converts fructose-6-phosphate to fructose-1,6-diphosphate. Patients with PFK deficiency (type VII glycogen storage disease, or Tarui's disease) have a clinical presentation similar to that of patients with myophosphorylase deficiency. The PFK stain is based on the conversion of exogenous fructose-6-phosphate to fructose-1,6-diphosphate by endogenous PFK. A metabolite of fructose-1,6-diphosphate – diphosphoglyceric acid – is formed *in vitro*, which then reacts with exogenous nicotinamide adenine dinucleotide to generate reduced nitro blue tetrazolium, the latter forming the usual blue precipitate. Sections are coverslipped using an organic mounting medium [1, 11, 17]. PFK is a labile enzyme that deteriorates rapidly in improperly handled biopsies. Patient sections stained for PFK should include a negative control (no added substrate) and a control section using fructose-1,6-diphosphate as a substrate, the latter always generating a blue reaction product, even if the patient is PFK-deficient. Patient sections stained for PFK activity should always be paired with a normal control section.

A final enzyme histochemical stain that is routinely performed in our laboratory is the ***myoadenylate deaminase (MAD) stain***. MAD is an enzyme that removes an ammonia molecule from adenosine monophosphate (AMP) to convert AMP to inosine monophosphate. Deficiency of the enzyme should be suspected when patients fail to generate a normal amount of ammonia during exercise testing. The clinical significance of MAD deficiency appears to vary from patient to patient. While some patients with MAD deficiency are asymptomatic, MAD deficiency has been associated in other patients with a clinical syndrome of exercise intolerance and exercise-induced muscle cramps and pain, and, in severe cases, rhabdomyolysis. A susceptibility to malignant hyperthermia syndrome has been suggested by some authors [25, 26]. The MAD stain is based on the generation of ammonia from an exogenous AMP substrate and subsequent reduction of nitro blue tetrazolium to form a blue reaction product. Staining for MAD is always paired with a negative control, in which aqueous citrate is added to the reaction in place of AMP substrate. Stained sections are coverslipped using an aqueous mounting medium [1, 18]. In patients with MAD deficiency, no blue reaction product is present in the sections stained with the AMP substrate. In addition to detecting MAD deficiency, the MAD stain reliably highlights tubular aggregates (see discussion of abnormal sarcoplasmic inclusions under "Interpretation of the Biopsy", below).

Non-enzymatic Staining of Fixed Skeletal Muscle (Paraffin Sections)

Although most of the useful diagnostic information in muscle biopsies at the light microscopic level is provided by the evaluation of stained cryostat sections, properly processed paraffin embedded tissue can also be of help in some conditions, particularly those characterized by the presence of inflammatory infiltrates and microorganisms. The morphology of inflammatory cells is generally better preserved in fixed, paraffin embedded tissue than in cryostat sections, and immunohistochemical markers (discussed below) often label inflammatory cells more clearly

in paraffin-embedded tissue than in frozen tissue. Paraffin sections of skeletal muscle biopsies are routinely stained with ***H&E***, ***Masson trichrome*** and ***Congo red*** stains in our laboratory. The H&E and Congo red stains have the same applications in paraffin sections as they do in cryostat sections. The Masson trichrome stain is a sensitive stain for highlighting connective tissue in paraffin sections. An additional stain, the ***Morin stain***, has proven to be helpful in the detection of aluminum deposits in patients with macrophagic myofasciitis (see discussion of cellular infiltrates under "Interpretation of the Biopsy", below) [27].

Immunohistochemical Stains

Immunohistochemical staining is a technique that allows one to localize specific proteins in tissue sections. The procedure has broad applications in all areas of anatomic pathology, and now plays an indispensable role in the evaluation of a wide range of muscle disorders [1, 28, 29]. In brief, immunohistochemical staining involves incubation of a tissue section with a primary antibody directed against the protein of interest, followed by incubation of the tissue with a secondary antibody that recognizes the primary immunoglobulin molecule and, finally, labeling the secondary antibody with a molecule that can be visualized under the microscope. Both fluorescent and non-fluorescent labels are commercially available. Technical aspects of immunohistochemical staining are presented in detail in other references [1], and will not be reviewed here. Automated procedures are now available for immunohistochemical staining, greatly improving turnaround time for this procedure.

Demonstration of many of the proteins of interest in the evaluation of skeletal muscle generally requires the use of frozen sections, although some recent work has suggested that paraffin embedded tissue may also be used for this purpose [30]. These include virtually all of the sarcolemmal proteins of interest in the evaluation of suspected muscular dystrophies, as well as major histocompatibility complex class I (MHC1) antigen and terminal complement complex ($C_{5b\text{-}9}$), the latter two stains of special importance in the evaluation of suspected inflammatory muscle diseases. Staining for MHC class I has been particularly valuable in identifying cases of inflammatory myopathy associated with minimal changes in routine frozen and paraffin sections. Patterns of abnormal MHC1 reactivity associated with inflammatory myopathies are illustrated in Fig. 1.9a, b. The abnormal protein aggregates that characterize some muscle diseases (e.g., myofibrillar myopathies) are also most reliably demonstrated in cryostat sections. Many of the more common inflammatory cell markers, in contrast, are better demonstrated in paraffin embedded tissue. The immunohistochemical markers commonly employed in our laboratory in the evaluation of muscle biopsies, the preferred tissue for staining and the significance of each of these markers, are listed in Table 1.1.

As in the cases of the enzyme histochemical stains discussed previously, it is essential that appropriate control sections be available whenever immunohistochemical staining is performed, in order to minimize the possibility of either false negative or

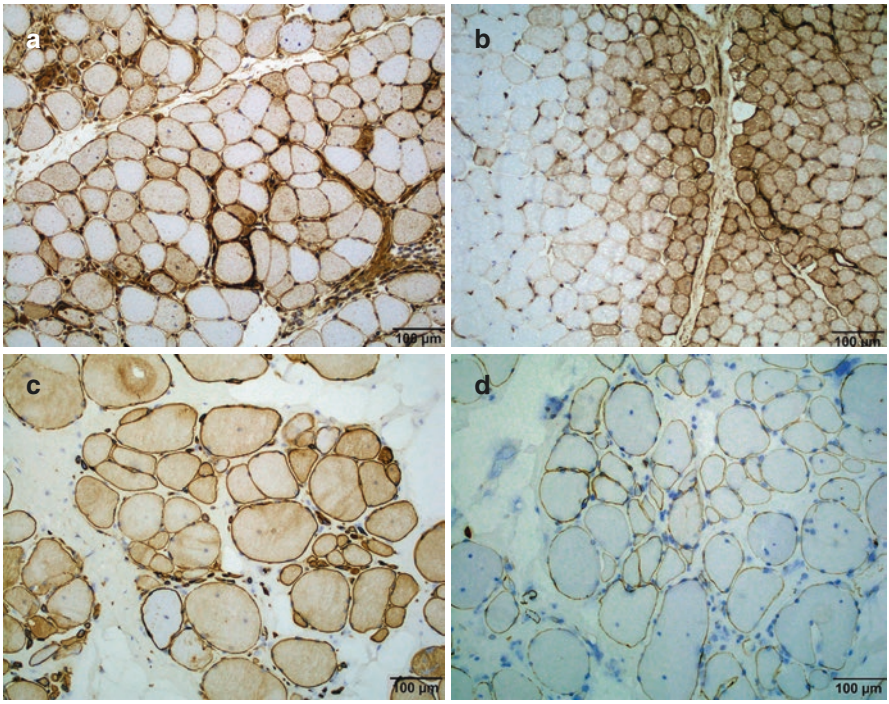

Fig. 1.9 Immunohistochemical staining of skeletal muscle. (**a**) Polymyositis, MHC class 1 (MHC1). MHC1 staining has been an invaluable tool in the assessment of suspected inflammatory myopathies. Sarcolemmal MCH1 reactivity can be seen in injured muscle fibers in a wide variety of conditions, but in classical polymyositis, one usually sees generalized reactivity involving both injured and morphologically normal fibers. Similar patterns of diffuse reactivity can be seen in inclusion body myositis and in some cases of dermatomyositis, related "overlap" inflammatory myopathic processes and in some dystrophies. (**b**) Dermatomyositis, MHC1. In many cases of dermatomyositis, one encounters selective staining of the sarcolemma in perifascicular myofibers, as shown here. In other patients with dermatomyositis, more diffuse sarcolemmal reactivity can be seen. (**c**) Becker muscular dystrophy, β-spectrin. When staining muscle biopsies for one of the dystrophy-associated membrane proteins, it is important to ensure that abnormalities in sarcolemmal staining are due to a specific protein abnormality rather than a nonspecific loss of membrane integrity due to cell injury or artifact. In this field, sarcolemmal β-spectrin reactivity is well preserved. (**d**) Becker muscular dystrophy, dystrophin carboxy terminus. In a contiguous section of the muscle biopsy shown in **c**, there is considerable loss of sarcolemmal dystrophin reactivity. The presence of intact β-spectrin staining in the same area ensures that the loss of dystrophin staining is caused by a true dystrophin abnormality rather than by nonspecific muscle fiber damage or an artifactual loss of immunoreactivity

false positive staining. These control sections should always include normal tissue stained for the protein of interest as well as negative controls. In addition, in the evaluation of sarcolemmal proteins in suspected muscular dystrophies, it is essential to ensure that the sarcolemma has not been artifactually disrupted by poor freezing technique or nonspecific myofiber injury. To accomplish this, sections stained for

Table 1.1 Antibodies, Preferred tissue, and Significance

Antibody	Preferred tissue	Significance
MHC class 1	Cryostat sections	Diffuse upregulation in polymyositis, inclusion body myositis, some cases of dermatomyositis; selective perifascicular upregulation in some cases of dermatomyositis
$C_{5b\text{-}9}$	Cryostat sections	Capillary reactivity seen in dermatomyositis, myopathy with pipestem capillaries, diabetes mellitus
β-spectrin	Cryostat sections	Essential control stain to ensure membrane integrity when evaluating muscle for sarcolemmal dystrophy-associated proteins
Dystrophin epitopes (rod domain, carboxy terminus, amino terminus)	Cryostat sections	Evaluation of suspected Duchenne / Becker dystrophy and other dystrophin-related disorders
Sarcoglycans (α, β, γ, δ)	Cryostat sections	Evaluation of suspected sarcoglycanopathies (LGMD∗ types 2C, 2D, 2E, 2F)
Caveolin-3	Cryostat sections	Evaluation of suspected LGMD∗ type 1C, rippling muscle disease, unexplained hyperCKemia
Dysferlin	Cryostat sections	Evaluation of suspected LGMD∗ type 2B, Miyoshi myopathy and related myopathies
α-dystroglycan	Cryostat sections	Evaluation of suspected congenital muscular dystrophies, LGMD∗ types 2I and 2M
Merosin (80 kDa and 300 kDa epitopes)	Cryostat sections	Evaluation of suspected merosin-deficient congenital muscular dystrophies
Collagen VI	Cryostat sections	Evaluation of suspected Ullrich or Bethlem myopathies
Collagen IV	Cryostat sections	Control stain for collagen VI staining
Emerin	Cryostat or paraffin sections	Evaluation of suspected Emery-Dreifuss muscular dystrophy
CD3	Paraffin sections	Pan T-lymphocyte marker
CD4	Paraffin sections	Helper T-lymphocyte marker
CD8	Paraffin sections	Cytotoxic/killer T-lymphocyte marker
CD20	Paraffin sections	B-lymphocyte marker
CD68	Paraffin sections	Macrophage marker
Desmin	Cryostat or paraffin sections	Evaluation of suspected myofibrillar myopathies
αB-crystallin	Cryostat or paraffin sections	Evaluation of suspected myofibrillar myopathies

[a]*LGMD* Limb Girdle Muscular Dystrophy

any dystrophy-associated sarcolemmal protein (e.g., dystrophin) should always be accompanied by patient sections stained in parallel for β-spectrin, a protein that is always present in the sarcolemma. The presence of intact β-spectrin reactivity in a given myofiber ensures that there has not been an artifactual or nonspecific disruption of the integrity of the sarcolemma. An example of normal β-spectrin staining and abnormal dystrophin staining in a patient with Becker muscular dystrophy is illustrated in Fig. 1.9c, d.

Electron Microscopy

Although less widely used in general pathology practice than in the past, electron microscopy continues to play a role in the evaluation of skeletal muscle biopsies. As noted in the section on the initial processing of skeletal muscle biopsies, electron microscopic evaluation of skeletal muscle is performed on fixed, resin-embedded tissue. In our laboratory, small sections of the same isometrically clamped, formalin-fixed muscle segment that is used for paraffin histology are post-fixed in glutaraldehyde and embedded in an Epon® medium. Delayed fixation or other improper handling of the biopsy can introduce significant artifacts into the tissue that hamper interpretation of fine structural changes. Prior to the preparation of thin sections for electron microscopy, 1.5 μm semithin sections of the tissue blocks are stained with toluidine blue and evaluated by light microscopy to select the optimum areas for ultrastructural study. Longitudinal sections of this tissue generally provide the most useful diagnostic information. Once an appropriate area has been identified in the semithin sections, thin (100 nm) sections are obtained from the block, placed on a copper grid, and stained with uranyl acetate-lead citrate [31]. The cross sectional area of the sections submitted for electron microscopy is quite small compared to the usual cryostat or paraffin sections, and sampling limitations should always be kept in mind when evaluating tissue ultrastructurally. Electron microscopy should never be used as a stand-alone diagnostic technique, but rather must be interpreted in the context of changes at the light microscopic level and the clinical history.

As in the case of the light microscopic evaluation of muscle biopsies, proper interpretation of changes at an ultrastructural level is based on a thorough knowledge of normal skeletal muscle morphology, particularly the appearance of the contractile apparatus (Fig. 1.10), sarcotubular structures, storage material, mitochondria, sarcolemma and nuclei. The observer should also be familiar with the appearance of surrounding connective tissue and the morphology of interstitial blood vessels.

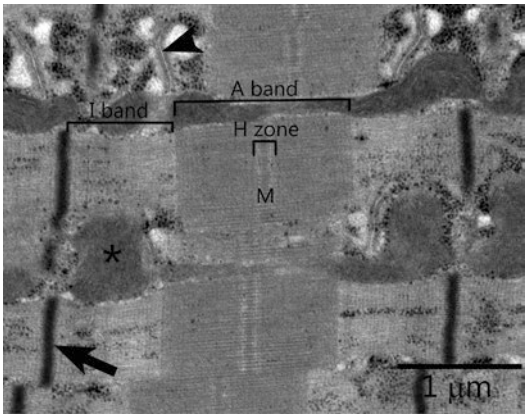

Fig. 1.10 Electron micrograph of normal sarcomeric structures. The sarcomere is the basic contractile unit of skeletal muscle, and familiarity with the appearance of normal sarcomeres is the foundation for interpreting the various structural abnormalities that one can see in diseased muscle. The normal sarcomere is bordered on each end by densely staining Z-bands (arrows), biochemically complex structures that contain a-actinin and a multitude of additional proteins, including those that anchor actin, titin and nebulin filaments. Immediately adjacent to the Z-band, one encounters a lightly-staining region known as the "isotropic" (I) band, composed of actin filaments and various accessory proteins (including nebulin and titin). The sarcomere's I-bands flank a darker staining area in the central region of the sarcomere known as the "anisotropic" (A) band, composed of myosin (thick) filaments, a number of accessory proteins and, at its junction with the I-band, variable numbers of overlapping actin filaments. In the center of each A-band, a lighter staining area called the H-zone is present, composed portions of the myosin filaments that are not overlapping with actin filaments. A central line (M) bisects the H-zone, composed of the creatine kinase and various proteins that anchor myosin filaments and cross-link proteins in the A-band on the other side of the M line. Mitochondria (∗) as well as T-tubules (arrowhead) and adjacent cisternae of sarcoplasmic reticulum are also visible in this field

Interpretation of the Biopsy

Proper interpretation of skeletal muscle biopsies begins, ideally, with familiarity with the patient's clinical history, including age, presenting symptoms, duration of disease, family history, imaging studies and any laboratory studies (e.g., CK levels). Clinical information may be lacking at the time biopsies are submitted to the laboratory, and in such cases, the pathologist should make every effort to contact the referring physician to obtain that information. Changes that should be noted in the biopsy include: (1) patterns of myofiber atrophy or hypertrophy; (2) the presence of myofiber degeneration, necrosis or regeneration; (3) changes in the location and appearance of myofiber nuclei and; (4) structural sarcoplasmic abnormalities, including sarcoplasmic whorling, myofiber myofibrillar disarray, inclusions and vacuolar change; (5) connective tissue changes; (6) abnormal cellular infiltrates and (7) alterations related to poor specimen preservation. These are discussed in more detail in the paragraphs below.

Myofiber Atrophy and Hypertrophy

The size and shape of individual myofibers should be noted and documented in the biopsy report. It is important to remember that myofiber size is influenced by the age of the patient, and myofiber diameters, particularly in pediatric patients, should be measured and compared to published normal ranges. ***Myofiber atrophy*** is a common alteration in muscle biopsies, occurring in disuse, denervation and many myopathic disorders. If atrophy is present, the ***shapes of the atrophic myofibers*** should be noted. Angular atrophic myofibers are typical in cases of denervation atrophy and most cases of type 2 myofiber atrophy in mature skeletal muscle (Fig. 1.11a), while more rounded atrophic fibers are typical of denervation in infants with spinal muscular atrophy type 1 (Fig. 1.11b) and in many myopathic processes. Profound myofiber atrophy, manifested by the presence of compact myonuclear clusters, is common in long-standing denervation, and can also be seen in some myopathic processes, notably myotonic dystrophy. The ***distribution of the atrophic myofibers*** should also be documented. The presence of groups of contiguous atrophic myofibers (group atrophy) is a feature of denervation atrophy (Fig. 1.11c), while the presence of selective atrophy of myofibers at the periphery of muscle fascicles (perifascicular atrophy) is a feature of dermatomyositis and several other related inflammatory myopathic disorders (Fig. 1.11d). The histochemical subtype(s) of the atrophic fibers should also be noted; as one might expect, the ATPase stains play a critical role in identifying the subtype(s) of the atrophic fibers. ***Selective atrophy of type 2 myofibers*** is a common change in skeletal muscle biopsies, typically associated with disuse atrophy and/or hypercortisolism (Fig. 1.12a). The atrophy in such cases preferentially involves type IIb myofibers; the reason for this selective involvement of fast twitch glycolytic fibers remains unclear. Selective atrophy of type 1 fibers is much less common than type 2 atrophy, but can be seen in patients with myotonic dystrophy type 1. Selective "smallness" of type 1 fibers is also a feature of congenital fiber type disproportion and many other congenital myopathies. The term "hypotrophy" is sometimes used to describe the small size of the myofibers in such cases, based on the notion that the affected fibers have not undergone atrophy, but rather never reached normal diameters (Fig. 1.12b). Mixed type 1 and type 2 atrophy is a feature of neurogenic atrophy (Fig. 1.12c), but is also present in biopsies of many primary myopathic processes. Widespread myofiber atrophy is also a feature of myopathy with thick filament loss; the atrophic fibers in such cases can be mistaken for denervated fibers, but are distinguished from denervated myofibers by a widespread loss of sarcoplasmic ATPase reactivity. ***Myofiber hypertrophy*** is a feature of many muscular dystrophies and other chronic myopathic diseases, and can also be seen in biopsies from individuals engaged in weight-bearing exercise and in some cases of chronic denervation. Paradoxically hypertrophic type 1 myofibers are common in the infantile pattern of denervation seen in spinal muscular atrophy type I (Fig. 1.12d).

Myofiber Degeneration, Necrosis and Regeneration

Muscle fiber degeneration, necrosis and regeneration are common in a wide range of primary myopathic disorders, including inflammatory myopathies and other immune-mediated myopathic processes, most types of muscular dystrophy, metabolic myopathies associated with acute myofiber injury, and many myopathies caused by exogenous myotoxic insults. The sarcoplasm of ***degenerating myofibers*** can appear hypercontracted, dense and homogeneously staining in H&E and Gomori trichrome-stained cryostat sections or can appear paler than the sarcoplasm of adjacent normal fibers (Fig. 1.13a). The delicate intermyofibrillar network seen in normal fibers is obscured in degenerating fibers. As degeneration proceeds to frank necrosis, the sarcoplasm

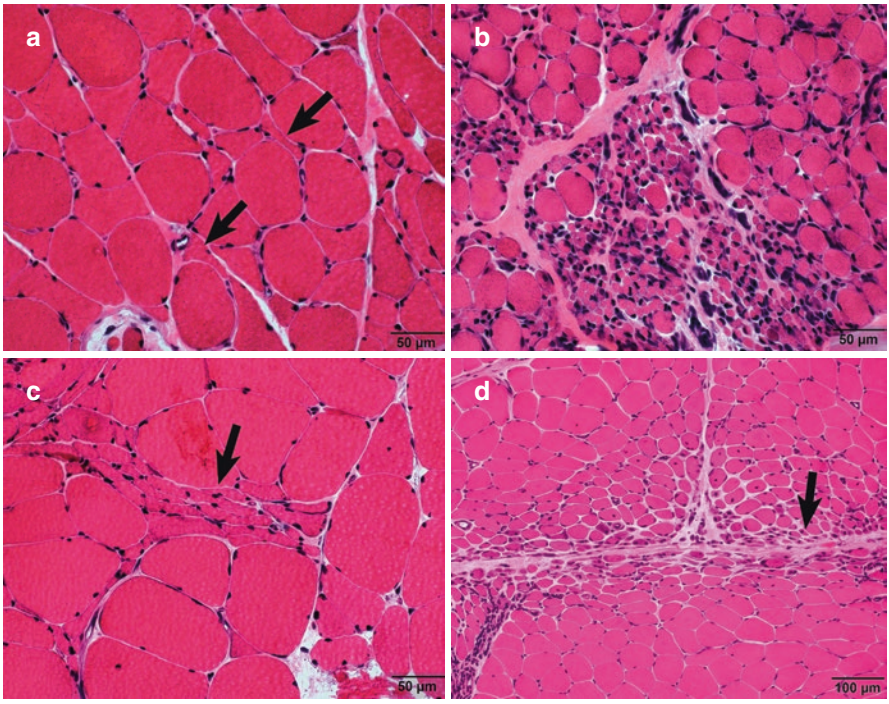

Fig. 1.11 Common patterns of myofiber atrophy. (**a**) Denervation atrophy, H&E. Neurogenic atrophy in mature skeletal muscle is characterized by the presence of atrophic myofibers with an angular profile in cross sections (arrow). This pattern can be difficult to distinguish from type 2 myofiber atrophy in H&E-stained sections. (**b**) Denervation atrophy in infancy, H&E. Denervation atrophy in young infants is characterized by the presence of groups of rounded, rather than angular, atrophic myofibers. This infantile pattern of denervation atrophy is seen most frequently in patients with infantile spinal muscular atrophy (SMA type 1). (**c**) Group atrophy in denervation atrophy, H&E. In many cases of denervation atrophy in mature muscle, angular atrophic myofibers occur in clusters, a pattern known as group atrophy (arrow). The presence of group atrophy helps one to distinguish denervation atrophy from type 2 myofiber atrophy even in H&E-stained sections. (**d**) Perifascicular atrophy in dermatomyositis, H&E. Selective atrophy of myofibers at the periphery of a muscle fascicle, termed perifascicular atrophy (arrow), is often seen in biopsies from patients with dermatomyositis and related inflammatory myopathic disorders (e.g. lupus myositis) (Panel **d** courtesy of Chunyu Cai, MD, PhD)

becomes fragmented, and is eventually invaded by macrophages, a process termed ***myophagocytosis*** (Fig. 1.13b). It is important to recognize that macrophagic invasion of such fibers is a nonspecific host reaction to the myofiber necrosis, and should not be interpreted as evidence of an inflammatory myopathic disorder (discussed below). The cytoplasm of ***regenerating myofibers***, in contrast, is basophilic, owing to the presence of sarcoplasmic ribonucleoproteins engaged in protein synthesis. The nuclei of regenerating myofiber tend to be enlarged, with finely dispersed chromatin and discernible nucleoli (Fig. 1.13c). It is not uncommon for regenerative change to occur in muscle fibers that contain residual necrotic sarcoplasm, the former typically manifesting as a rim of basophilic sarcoplasm at the edge of a central area of necrosis (Fig. 1.13d).

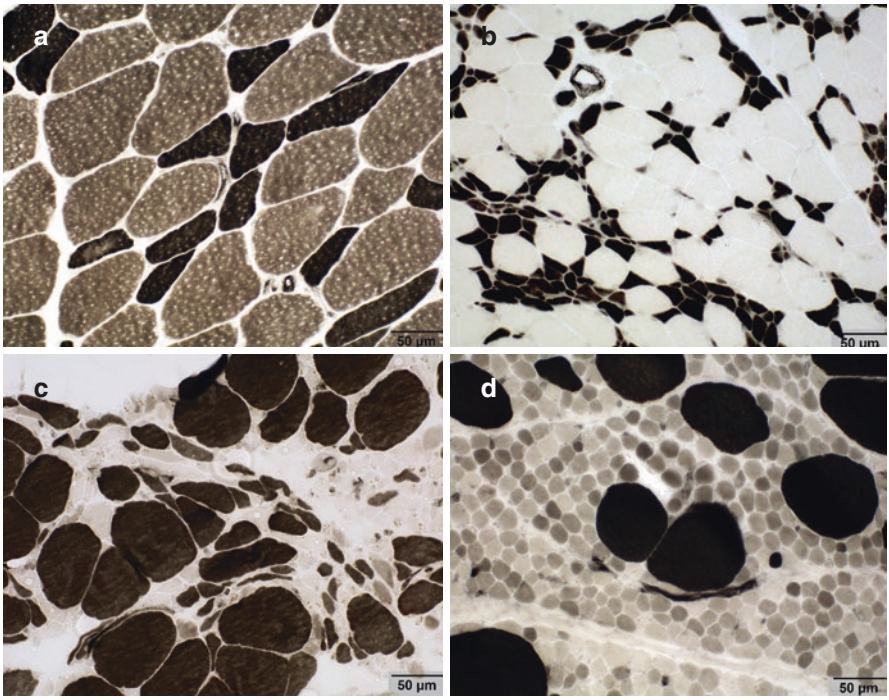

Fig. 1.12 Fiber type-specific patterns of myofiber atrophy and hypertrophy. (**a**) ATPase 9.4, type 2 myofiber atrophy. Selective atrophy of type 2 myofibers is a very common pattern of myofiber atrophy. Common clinical features in most of the long list of conditions associated with type 2 atrophy are disuse and elevated corticosteroid levels. (**b**) Type 1 myofiber atrophy/hypotrophy, ATPase 4.3. Selective "smallness" of type 1 myofibers is less common than selective type 2 myofiber atrophy. It is most commonly encountered in congenital fiber size disproportion and other congenital myopathic disorders where it is usually referred to as "hypotrophy" rather than atrophy, based on the assumption that the fibers have never reached a normal diameter during their development. Small type 1 fibers are also often present in biopsies from patients with myotonic dystrophy, type 1. (**c**) Denervation atrophy, ATPase 4.3. Mixed type 1 and type 2 myofiber atrophy is a characteristic feature of neurogenic atrophy. It is also common in many myopathic disorders, but in the latter conditions, the affected fibers are usually rounded rather than angular. (**d**) Infantile spinal muscular atrophy, ATPase 4.3. Myofiber hypertrophy involving both type 1 and type 2 fibers is commonly seen in chronic myopathic processes as well as in many cases of chronic neurogenic atrophy. Selective type 1 myofiber hypertrophy, illustrated here, is usually present in biopsies from infants with SMA type 1

Changes in the Location and Appearance of Myofiber Nuclei

As noted previously and illustrated earlier in Fig. 1.3, myofiber nuclei normally lie just beneath the sarcolemma. ***Increased numbers of internalized nuclei*** – defined by the presence of internalized nuclei in >3% of myofibers in transverse of areas away from myotendinous insertion sites – are common in many chronic myopathic and neuropathic disorders, where they usually coexist with myofiber hypertrophy, myofiber splitting and other chronic sarcoplasmic alterations discussed in the next section. Internalized nuclei are also common in regenerating muscle fibers. Internalized – often centrally-situated - nuclei are a defining feature of the ***centronuclear myopathies***, a genetically and clinically heterogeneous group of congenital myopathies with presentations that range from severe neonatal weakness with respiratory failure and early death - e.g. X-linked myotubular myopathy (Fig. 1.14a) - to adult-onset, much more slowly progressive weakness. A number of genetic abnormalities, variably associated with X-linked, autosomal dominant or autosomal recessive inheritance patterns, have been described [32]. Mutations in the gene encoding the ryanodine receptor, best known for its association with central core disease and susceptibility to malignant hyperthermia syndrome, have also been associated with abnormal numbers of central / internalized nuclei [33]. Internal nuclei are also a common feature of ***myotonic dystrophy***, particularly myotonic dystrophy type 1 (DM1) (Fig. 1.14b). Biopsies from patients with congenital-onset DM1 may be extremely difficult to distinguish from those with congenital onset variants of centronuclear myopathy [34].

Changes in the appearance of myofiber nuclei should also be noted in the biopsy report. As mentioned previously, ***enlarged nuclei*** with finely dispersed chromatin and conspicuous nucleoli are a feature of myofiber regeneration. Although difficult to appreciate at the light microscopic level, a number of different ***intranuclear inclusions*** can be seen under the electron microscope in a number of different neuromuscular disorders, including inclusion body myositis [35], oculopharyngeal muscular dystrophy [36], inflammatory myopathies associated with the presence of anti-synthetase antibodies [37] and some cases of nemaline myopathy [38] (see discussion of “nemaline bodies” under Abnormal Sarcoplasmic Inclusions, below).

Sarcoplasmic Abnormalities

A wide variety of other sarcoplasmic structural alterations can be seen in muscle biopsies. These include (1) various forms of ***myofibrillar disarray***, (2) abnormal ***sarcoplasmic inclusions*** and (3) ***vacuolar change***.

Patterns of myofibrillar disarray include myofiber splitting, sarcoplasmic “whorling”, target/targetoid change, central cores, multiminicores, ring fibers, lobulated (trabecular) change, moth-eaten change and whorled fibers. Target/targetoid change and sarcoplasmic cores are similar from a morphological standpoint but have very different clinical implications. ***Myofiber splitting*** is particularly common in hypertrophic fibers (Fig. 1.15a), and is a feature of chronic myopathic and some

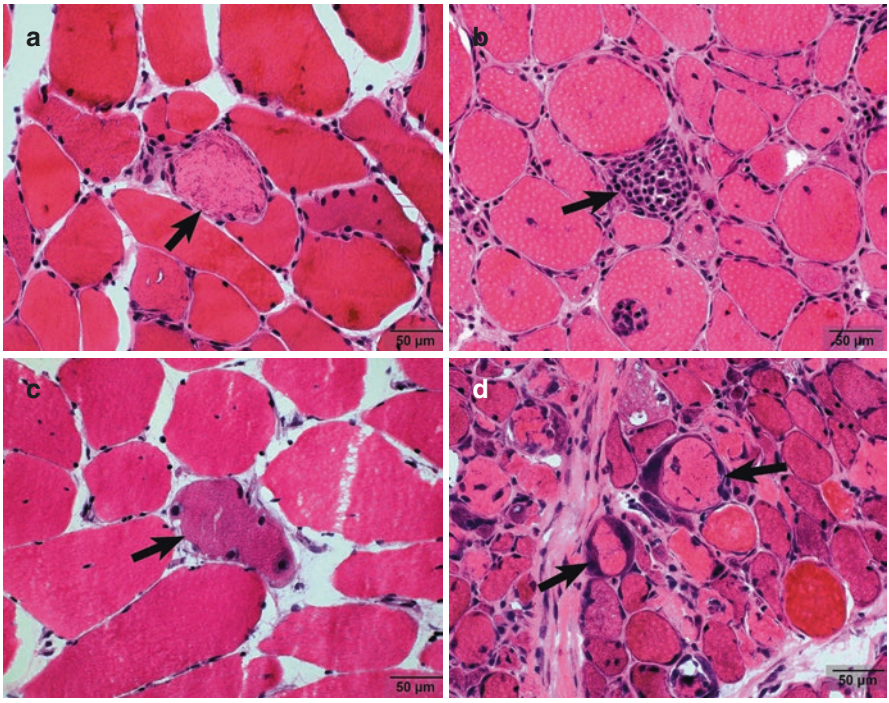

Fig. 1.13 Myofiber degeneration, necrosis and regeneration. (**a**) Degenerating myofiber, H&E. As myofibers degenerate, their sarcoplasm often becomes pale (arrow) and the normal intermyofibrillar network is obscured. In other instances, the sarcoplasm of degenerating myofibers can stain more darkly than that of normal myofibers due to the presence of denatured proteins. (**b**) Myophagocytosis, H&E. Once a myofiber becomes necrotic, its sarcoplasm becomes fragmented and undergoes phagocytosis by macrophages (arrow). (**c**) Regenerating myofiber, H&E. The sarcoplasm of regenerating myofibers is basophilic (arrow), owing to the presence of ribonucleoproteins engaged in protein synthesis. The nuclei of regenerating myofibers are enlarged, and often contain conspicuous nucleoli. (**d**) H&E, mixed myofiber necrosis and regeneration. Myofiber necrosis and regeneration often occur as segmental changes, and it is not uncommon to see evidence of regenerative sarcoplasmic basophilia (arrow) adjacent to areas of sarcoplasmic necrosis in the same myofiber

neuropathic conditions. Split fibers are also a normal feature of myotendinous insertion sites, and in this location should not be interpreted as evidence of a myopathic disorder. Myofiber splitting is often accompanied by other chronic architectural abnormalities, including increased numbers of internalized nuclei, internalized capillary loops, and irregular areas of sarcomeric disarray, the last imparting a *"whorled"* appearance to the sarcoplasm of affected fibers in transverse sections (Fig. 1.15b). This pattern of sarcomeric disarray is common in dystrophic processes, but can also be seen in long-standing chronic neurogenic disorders. The NADH-TR stain, as noted earlier, is a useful stain for demonstrating a number of important sarcoplasmic abnormalities. ***Target/targetoid change*** is characterized by the presence of a fairly well-demarcated zone of pallor and decreased oxidative enzyme activity caused by disorganization of sarcomeres and an absence of mitochondria,

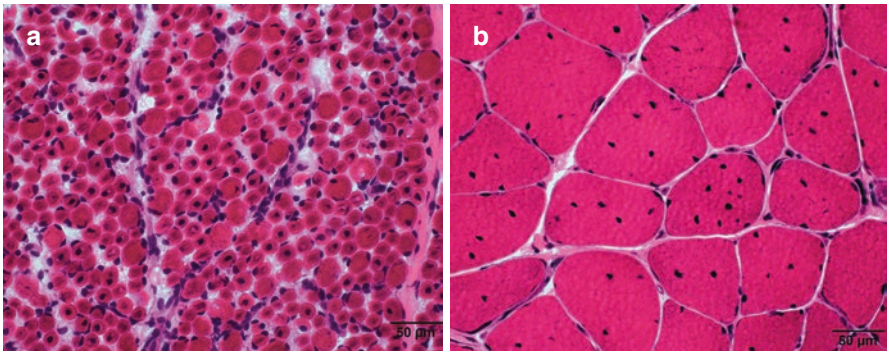

Fig. 1.14 Abnormalities in the location of myofiber nuclei. (**a**) H&E, X-linked myotubular myopathy. In normal skeletal muscle in both infants and older individuals, the vast majority of the myofiber nuclei lie just beneath the sarcolemma. Internalized nuclei are common near myotendinous insertion sites in normal muscle, and are also common in chronic myopathic and neuropathic processes. X-linked myotubular myopathy, illustrated here, is one of a group of hereditary congenital myopathies characterized by abnormally increased numbers of centrally-situated nuclei. (**b**) Myotonic dystrophy type 1, H&E. Myotonic dystrophy is another form of hereditary myopathy associated with increased numbers of internalized nuclei. In biopsies from older patients with this condition, a significant number of myofibers contain multiple, randomly distributed internalized nuclei. In cases of myotonic dystrophy presenting in infancy, the histological changes may be difficult to distinguish from myotubular myopathy and other congenital centronuclear myopathies

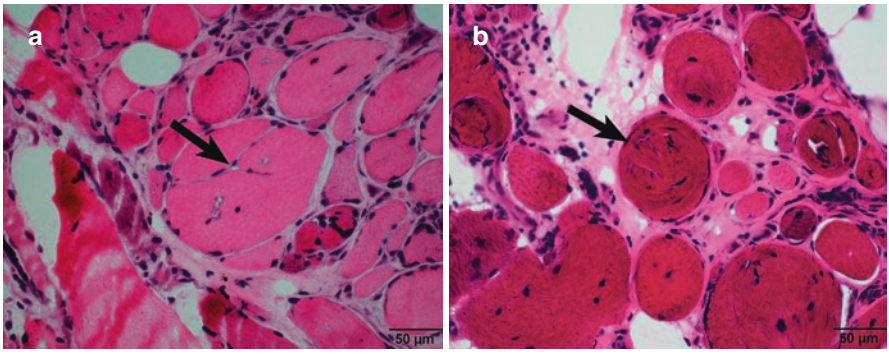

Fig. 1.15 Patterns of myofibrillar disarray: myofiber splitting and sarcoplasmic "whorling". (**a**) Myofiber splitting, H&E. Myofiber splitting is a common, nonspecific change in chronic myopathic disorders, and can also be seen as a secondary change in chronic neurogenic atrophy. The "splitting" (arrow) typically occurs in hypertrophic fibers, and is associated with the presence of internalized nuclei and, in some cases, internalized capillary loops. (**b**) Sarcoplasmic whorling, H&E. "Whorling" of sarcoplasmic elements (arrow) is another common change seen in a wide range of chronic myopathic conditions. Like myofiber splitting, with which it usually coexists, this pattern of sarcomeric disarray is most common in hypertrophic myofibers and is associated with internalized nuclei

usually near the center of the myofiber in transverse sections. Target fibers are distinguished from targetoid fibers by the presence of a thin zone of increased oxidative enzyme activity at the edge of the region of decreased oxidative enzyme activity, while "targetoid" fibers lack this hyperintense border. Both of these structures are best visualized in NADH-TR-stained cryostat sections (Fig. 1.16a) and in sections stained for mitochondrial enzyme activity. Target formation is usually restricted to type I myofibers and is most commonly seen in chronic denervation, although it can also be produced by tendon transection. At an ultrastructural level, targets extend for a considerable distance along the long axis of the affected fiber and are characterized by an absence of mitochondria and variable degrees of sarcomeric disarray and Z-band streaming. Sarcoplasmic cores are another important pattern of myofibrillar disarray, and can take the form of central cores or so-called multiminicores (also known as minicores). As the name suggests, ***central cores*** are classically located in the central area of the sarcoplasm of transversely sectioned fibers, but can also occupy a more eccentric position. Like target fibers, cores are characterized by a well-demarcated zone of decreased oxidative enzyme activity (Fig. 1.16b). They are the defining morphological feature of central core disease, a congenital myopathy associated in a significant number of patients with a ryanodine receptor (RYR1) mutation and susceptibility to malignant hyperthermia syndrome [39]. Like target fibers, their distribution is limited to type I fibers. Ultrastructurally, two forms of central cores have been described. The so-called unstructured cores are characterized by sarcomeric disarray and Z-band streaming similar to that seen in target fibers. "Structured" cores, on the other hand, are characterized by the presence of readily discernable sarcomeres that are usually shorter than the sarcomeres in the adjacent non-core areas and contain wider, more irregular Z-bands. ***Multiminicores*** are also characterized by zones of decreased oxidative enzyme activity but, unlike targets and central cores, tend to be multiple and smaller (Fig. 1.16c), with an orientation perpendicular to the long axis of the affected myofiber. Multiminicores are a feature of a family of congenital myopathies known as multiminicore (or multicore) myopathies. A significant percentage of cases of congenital myopathies with a multiminicore morphology have been associated with a mutation in the gene encoding selenoprotein N1, although other variants also occur. Although not initially felt to be associated with a risk of malignant hyperthermia, some patients with multiminicore change have been shown to carry a mutation in the RYR1 gene and, with it, susceptibility to malignant hyperthermia syndrome [40]. Although uncommon, multiminicore-like structures can also occasionally be encountered in patients with chronic denervation. ***Moth-eaten change*** is a common, nonspecific change that is also characterized by the presence of irregular areas of decreased oxidative enzyme activity (Fig. 1.16f). Moth-eaten change can be difficult to distinguish from multiminicores in some cases. ***Lobulated*** (or ***trabecular***) fibers are myofibers that have an abnormally coarsely-staining intermyofibrillar network that is also best demonstrated in the NADH-TR stain (Fig. 1.17a). This pattern is caused by abnormal aggregation of mitochondria, thought to be associated with a defect in the nor-

mal "anchoring" of mitochondria near Z-bands. The lobulated change typically preferentially affects type 1 myofibers, which are often atrophic. While not specific for any one myopathic disorder, they are particularly common in patients with the autosomal recessive form of limb girdle muscular dystrophy associated with

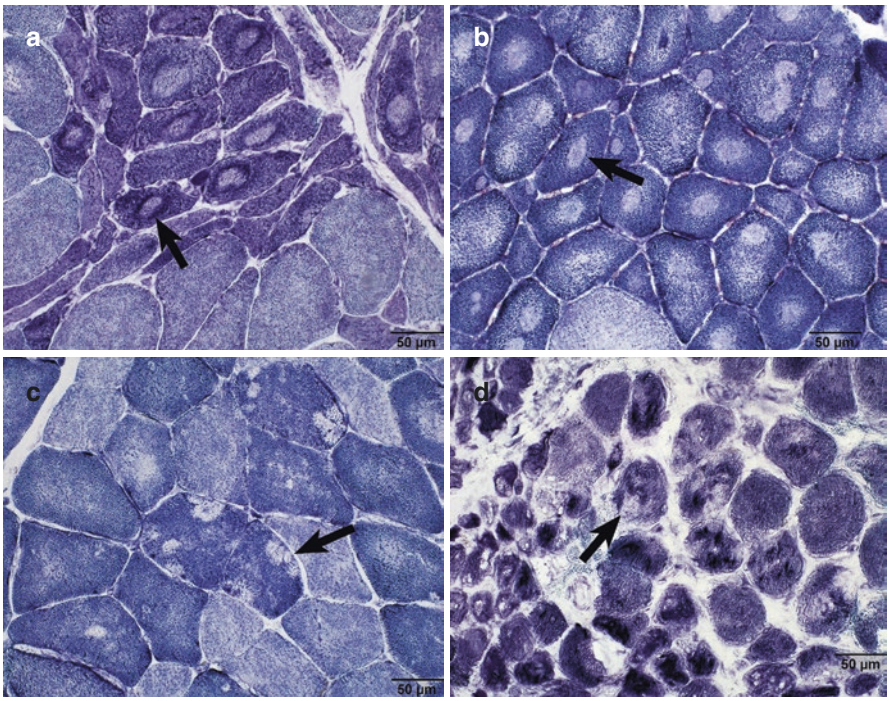

Fig. 1.16 Patterns of myofibrillar disarray, continued: target/targetoid fibers, central cores, multiminicores and moth-eaten change. (**a**) Target fibers in chronic denervation, NADH-TR. The NADH-TR stain is an excellent stain for highlighting abnormalities in myofibrillar elements. Target fibers are common in chronic peripheral neuropathies, and are characterized by a fairly well-demarcated zone of decreased oxidative enzyme activity surrounded by a rim of increased enzyme activity (arrow). "Targetoid" fibers are similar to target fibers, but lack the peripheral zone of increased enzyme activity. (**b**) Central core disease, NADH-TR. Central cores, the hallmark of central core disease, are also best seen in oxidative stains, where they appear as a well-defined area of decreased enzyme activity (arrow). Despite their name, in some myofibers, the cores can lie in a more peripheral position. Patients with central cores are at increased risk for ryanodine receptor abnormalities and susceptibility to malignant hyperthermia syndrome. (**c**) Multiminicore disease, NADH-TR. Multiminicores, as the name suggests, appear as multiple, irregular areas of decreased oxidative enzyme activity (arrow). Multiminicore disease, although not originally felt to be associated with an increased risk of malignant hyperthermia syndrome, can also be associated with ryanodine receptor abnormalities. (**d**) Moth-eaten change, NADH-TR. Moth-eaten change refers to the presence of irregular, usually ill-defined areas of decreased oxidative enzyme activity (arrow) This is a nonspecific degenerative alteration encountered in a wide range of myopathic processes. Moth-eaten change can be difficult to distinguish from multiminicores, but is usually less widely distributed than the multiminicores seen in cases of multiminicore myopathy

calpain-3 deficiency (LGMD 2A) [41, 42]. They have also been reported in other dystrophic processes, including facioscapulohumeral dystrophy, and have been described as the predominant change in a subset of elderly patients with limb girdle weakness in the absence of a defined protein abnormality [43]. ***Ring fibers*** are another example of myofibrillar disarray, characterized by the presence of a peripheral rim of improperly oriented myofibrils encircling a central region of well-preserved sarcoplasm, best demonstrated in oxidative (Fig. 1.17b) and PAS stains. Ring fibers are often smaller and stain more intensely in H&E and Gomori trichrome stains than their normal counterparts. Although commonly associated with myotonic dystrophy, they can be seen in a wide range of myopathic processes, and sometimes as isolated incidental changes.

Abnormal sarcoplasmic inclusions can occur in muscle fibers, and their presence can provide important clues to the nature of the neuromuscular disorder. Many of these are recognizable in Gomori trichrome-stained cryostat sections, supplemented by other stains. ***Ragged red change*** in the Gomori trichrome stain is a hallmark of abnormal mitochondrial accumulation. As mentioned previously, the mitochondrial aggregates have a granular, faintly basophilic appearance in H&E sections. The membrane-rich mitochondria are highlighted red in the Gomori trichrome stain, producing the characteristic ragged red appearance (Fig. 1.18a). Mitochondrial stains, particularly the SDH stain, highlight mitochondrial aggregates with even greater sensitivity than the trichrome stain, and should always be

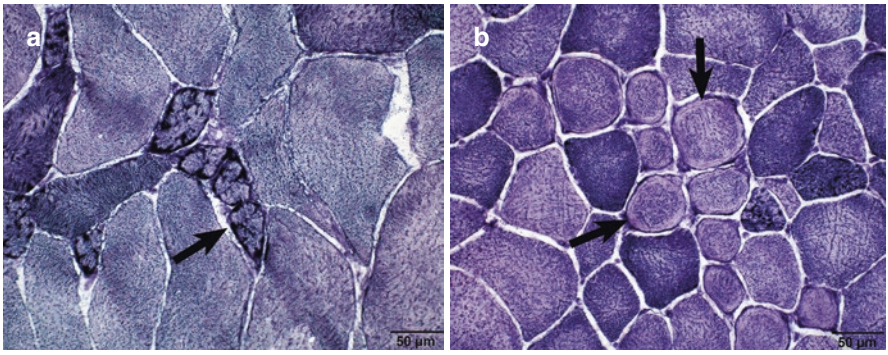

Fig. 1.17 Patterns of myofibrillar disarray, continued: lobulated fibers and ring fibers. (**a**) Lobulated fibers, NADH-TR. Lobulated fibers (arrow), sometimes designated as "trabecular" fibers, are characterized by coarsening of the intermyofibrillar network, best appreciated in oxidative stains. Lobulated fibers can be seen in a number of different myopathic disorders, and are often conspicuous in patients with facioscapulohumeral muscular dystrophy and in autosomal recessive limb girdle muscular dystrophy caused by calpain-3 deficiency (LGMD 2A). They have also been described as the predominant change in a subset of elderly patients with limb girdle weakness in the absence of a defined protein abnormality. The affected fibers are usually type 1 myofibers, and are smaller than neighboring normal myofibers. (**b**) Ring fibers, NADH-TR. Ring fibers, sometimes designated as spiral annulets or "Ringbinden", are characterized by a peripheral zone of circumferentially-oriented myofibrils (arrow) surrounding a central area of normally oriented myofibrils. They are most commonly seen in patients with myotonic dystrophy, but can be encountered as nonspecific changes in a wide range of chronic myopathic processes

used to confirm the mitochondrial nature of the inclusions. Ragged red change is also a feature of some inflammatory myopathies (inclusion body myositis [35, 44], polymyositis with COX-deficient myofibers [45], and is common in paraspinous muscles [46] and in muscle biopsies from older adults [47]. ***Tubular aggregates*** are membrane rich inclusions derived from redundant collections of sarcoplasmic reticulum that are also highlighted in the trichrome stain (Fig. 1.18b). These inclusions are sometimes mistaken for ragged red change, but tend to be better-demarcated than the mitochondrial aggregates in ragged red fibers. Like mitochondrial aggregates, they are highlighted in NADH-TR stained sections, but lack SDH and COX activity and, in contrast to mitochondrial aggregates, are typically restricted to type 2 myofibers (except in some of the rare familial tubular aggregate myopathies, in which they occur in type 1 fibers). Tubular aggregates are usually sporadic, incidental findings, but have also been associated with a number myopathic conditions, including some forms of periodic paralysis and myotonia [48]. Hereditary forms of tubular aggregate myopathy have also been documented, with symptoms that include progressive weakness, exercise-induced myalgias and cramps, and weakness with myasthenic features. In addition to highlighting membrane-rich sarcoplasmic accumulations, the Gomori trichrome stain is also useful for highlighting a variety of protein-rich inclusions. ***Nemaline bodies*** are a feature of the nemaline myopathies, a clinically and genetically heterogeneous group of congenital myopathies that are characterized by the presence of small rod-like structures (nemaline "rods") in the sarcoplasm of affected myofibers [49]. These structures contain a high concentration of the Z-disc protein α-actinin, stain dark-red to blue in the Gomori trichrome stain, and often aggregate at the periphery of the affected myofiber (Fig. 1.19a). Nemaline bodies can be difficult to identify at the light microscopic level in some biopsies, for which reason we routinely perform electron microscopy on any biopsy in which a nemaline myopathy (or other congenital myopathy) is suspected. Nemaline bodies can also be seen as incidental structures, particularly in the vicinity of myotendinous insertion sites and in extraocular muscles. ***Cytoplasmic bodies*** are fairly distinctive inclusions that are especially common in patients with inclusion body myopathies and myofibrillar myopathies (discussed below) [50]. They have been described in earlier publications as a distinguishing feature of a heterogeneous group of conditions termed "cytoplasmic body myopathies", some examples of which are now classified as variants of myofibrillar myopathy or inclusion body myopathy. They can also be encountered in patients with myopathy related to ipecac abuse [51] and as incidental findings in otherwise normal muscle. Cytoplasmic bodies are eosinophilic in H&E stained sections, and stain red to dark green in the Gomori trichrome stain (Fig. 1.19b); a pale halo is usually discernable at their periphery. They have a very distinctive ultrastructural appearance, with a darkly staining, dense filamentous core surrounded by a halo of thin radiating filaments. ***Spheroid bodies*** are another type of proteinaceous inclusion that can be seen in many of the same conditions that are associated with cytoplasmic bodies. They tend to be larger and more irregular than classical cytoplasmic bodies, but can be probably be thought of as a variant of the latter. Spheroid bodies are particularly conspicuous in spheroid body myopathy, a variant of myofibrillar myopathy associated with

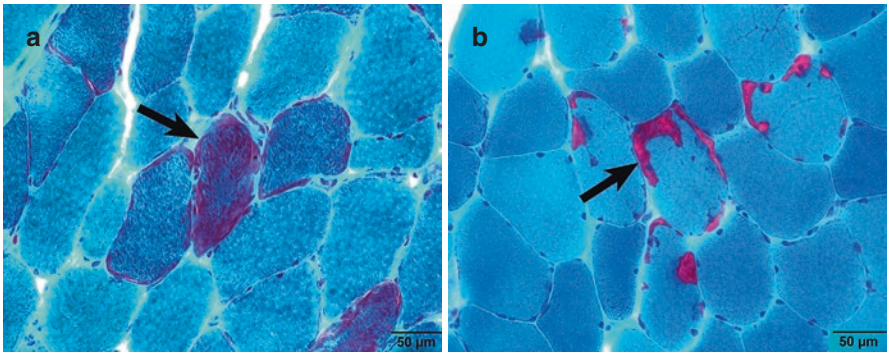

Fig. 1.18 Abnormal sarcoplasmic inclusions: ragged red change and tubular aggregates. (**a**) Ragged red change, Gomori trichrome. The Gomori trichrome stain is an invaluable tool for demonstrating a variety of abnormal sarcoplasmic inclusions. One of the best known examples is ragged red change (arrow), caused by the presence of abnormal mitochondrial aggregates. Such changes are the hallmark of many mitochondrial myopathies, but are also common in inclusion body myositis, polymyositis with mitochondrial abnormalities, in muscle biopsies from elderly patients, and in orbital and paraspinous muscles. Myofibers with ragged red change are also reliably highlighted in sections stained for succinate dehydrogenase activity. (**b**) Tubular aggregates, Gomori trichrome. Tubular aggregates (arrow) are structures composed of redundant collections of sarcoplasmic reticulum. Like mitochondrial membranes, the sarcoplasmic reticulum has an affinity for the red dye used in the Gomori trichrome stain. Tubular aggregates are sometimes confused with ragged red change, but tend to be better demarcated and, unlike ragged red change, usually restricted to type 2 fibers. They are NADH-TR reactive but lack mitochondrial enzyme activity

mutations in the gene encoding myotilin [52]. ***Reducing bodies*** are well-circumscribed, darkly-staining eosinophilic inclusions in H&E-stained sections that, like cytoplasmic bodies, stain dark red in the Gomori trichrome stain. They are distinguished from the latter by their dark reaction product in the menadione nitroblue tetrazolium stain [53]. Reducing bodies are a prominent feature in reducing body myopathies, hereditary myopathies caused by mutations in the *FHL1* gene [54]. Some myopathic disorders, exemplified by the myofibrillar myopathies, are characterized by the presence of ***larger, irregular proteinaceous aggregates***. The staining properties of these aggregates is variable, but most appear as irregular eosinophilic hyaline deposits in H&E sections (Fig. 1.19c). The inclusions can range from dark green to red in color in trichrome-stained cryostat sections, and in some cases stain faintly in Congo red stains. In the case of myofibrillar myopathies, the inclusions are often immunoreactive for desmin (Fig. 1.19d), as well as a number of other proteins [55, 56]. Abnormal proteinaceous aggregates are also a feature of sporadic inclusion body myositis [57] and hereditary inclusion body myopathies [58].

Sarcoplasmic vacuoles of various types are a feature of a number of different muscle diseases and, in some cases, are the defining feature of a specific myopathic disorder. One must be careful to distinguish true sarcoplasmic vacuoles from clear spaces caused by ice crystal artifact. Some vacuoles are distinguished by conspicuous ***lysosomal activity***, best demonstrated in cryostat sections stained for acid phosphatase activity. These include acid maltase deficiency (type II glycogen storage disease) (Fig. 1.20a, b) and two hereditary X-linked conditions (Danon myopathy,

associated with deficiency of the LAMP-2 protein [59], and X-linked myopathy with excessive autophagy [60, 61]. Vacuolar change and increased lysosomal activity are also a feature of some amphiphilic cationic myopathies, most notably those associated with exposure to chloroquine or hydroxychloroquine. ***Rimmed sarcoplasmic vacuoles*** are a feature of hereditary and sporadic inclusion body myopathies, myofibrillar myopathies, oculopharyngeal muscular dystrophy and some forms of hereditary limb girdle muscular dystrophy and distal myopathy. Classical rimmed vacuoles contain membranous material that is highlighted in the Gomori

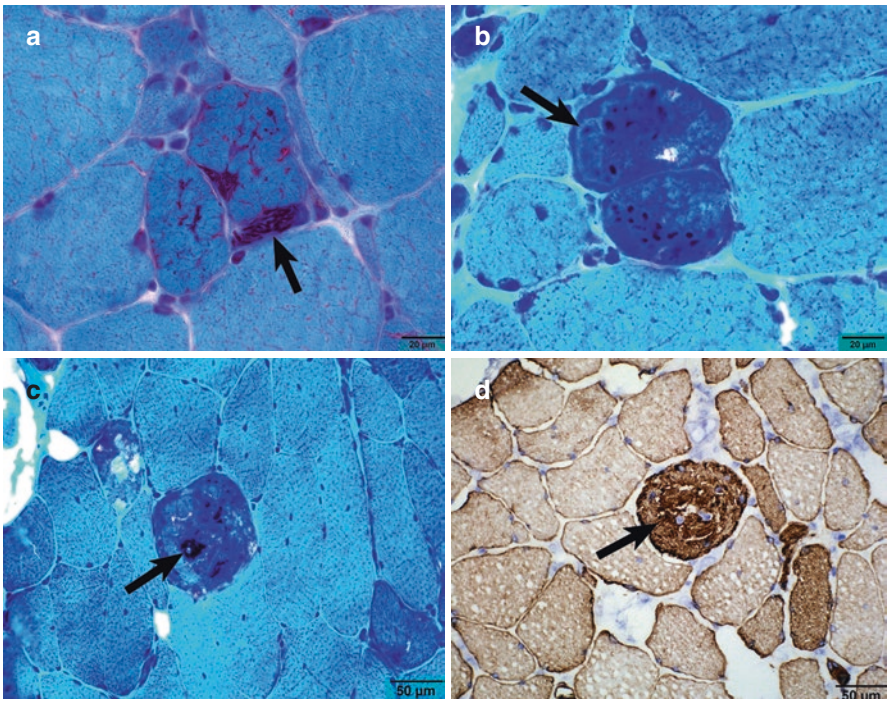

Fig. 1.19 Abnormal sarcoplasmic inclusions, continued: nemaline rods, cytoplasmic bodies and other proteinaceous aggregates. (**a**) Nemaline myopathy, Gomori trichrome. Nemaline rods are structures that are derived from abnormal sarcomeric Z-band material. They are the defining morphological feature of a clinically and genetically heterogeneous group of congenital myopathies known as nemaline myopathies. They can also be seen as incidental structures in a number of other myopathic processes and in normal skeletal muscle at myotendinous insertion sites. Nemaline rods typically cluster in subsarcolemmal areas (arrow). (**b**) Cytoplasmic bodies, Gomori trichrome. Cytoplasmic bodies are small proteinaceous inclusions that can be seen in a number of different myopathies, but are especially conspicuous in myofibrillar myopathies and inclusion body myopathies. The classic cytoplasmic body has a core that stains blue in the Gomori trichrome stain, surrounded by a clear halo (arrow). (**c**) Protein aggregate in myofibrillar myopathy, Gomori trichrome. Large, irregular proteinaceous inclusions, like cytoplasmic bodies, are common in myofibrillar myopathies and inclusion body myopathies. Their appearance ranges from red to blue-green in the Gomori trichrome stain (arrow). (**d**) Protein aggregate in myofibrillar myopathy, desmin stain. Immunohistochemical staining is a useful technique for identifying specific protein entities in the proteinaceous deposits seen in the trichrome stain. Desmin reactivity (arrow) is particularly common, although a variety of other proteins are often also present

trichrome stain, and gives the vacuoles their classical "rimmed" appearance (Fig. 1.20c). They are of lysosomal origin, and often have some acid phosphatase reactivity, although this is typically less intense than that seen in vacuoles in acid maltase deficiency. Amyloid is demonstrable in some examples, but this is variable. At an ultrastructural level, the rimmed vacuoles of inclusion body myositis contain bundles of characteristic "tubulofilamentous" structures measuring from 16–24 nm in diameter (Fig. 1.20d), usually accompanied by nonspecific lysosomal debris; accurate measurement of these tubulofilamentous structures is essential to avoid

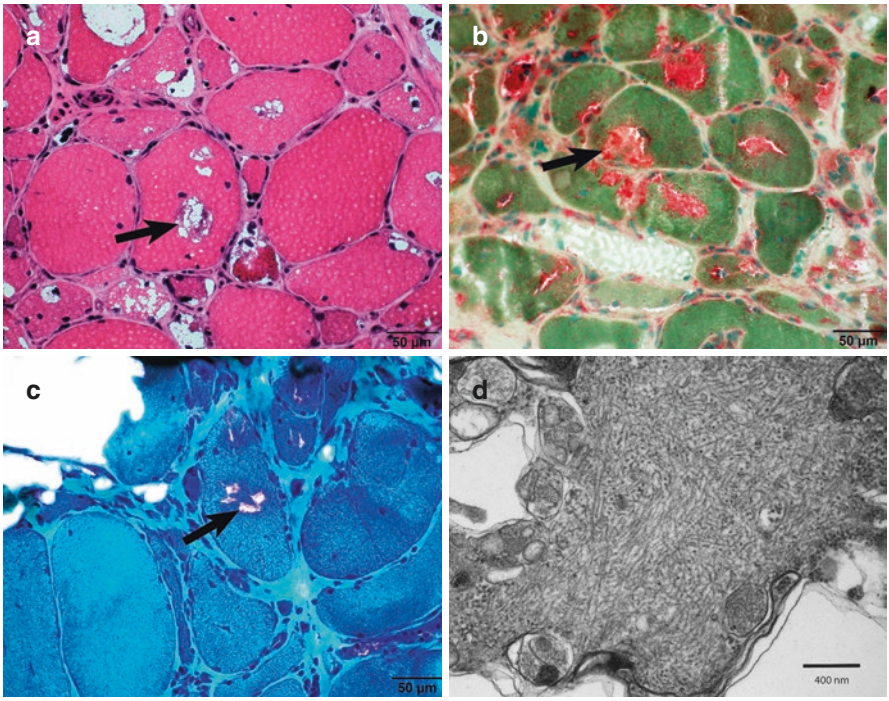

Fig. 1.20 Sarcoplasmic vacuoles: Acid maltase deficiency and inclusion body myositis. (**a**) Acid maltase deficiency, H&E. Acid maltase deficiency, also known as glycogen storage disease type 2, is characterized by the presence of vacuolar change (arrow). In adult cases, the vacuolar change is less dramatic than those seen in infantile cases (Pompe disease), and can vary considerably from muscle to muscle. The vacuoles contain stainable glycogen. (**b**) Acid maltase deficiency, acid phosphatase. In acid maltase deficiency, much of the abnormal glycogen accumulates within lysosomes, and is therefore associated with areas of abnormal acid phosphatase reactivity (arrow). Similar patterns of vacuolar change associated with abnormal lysosomal activity can also be seen in Danon myopathy and X-linked myopathy with excess autophagy. (**c**) Inclusion body myositis, Gomori trichrome. Rimmed vacuoles (arrow) are a characteristic feature of sporadic inclusion body myositis, hereditary inclusion body myopathies, myofibrillar myopathies, oculopharyngeal muscular dystrophy and some distal myopathies. The vacuoles typically contain abundant membranous debris, as well as an interesting array of proteins. The membranous debris has an affinity for the red dye in the Gomori trichrome stain. (**d**) Inclusion body myositis, EM. Under the electron microscope, the rimmed vacuoles in muscles from patients with inclusion body myositis often contain inclusions composed of filaments with diameters ranging from 16 to 24 mm. It is important to distinguish these larger filaments from collections of smaller actin and myosin filaments that can be seen in any injured myofiber

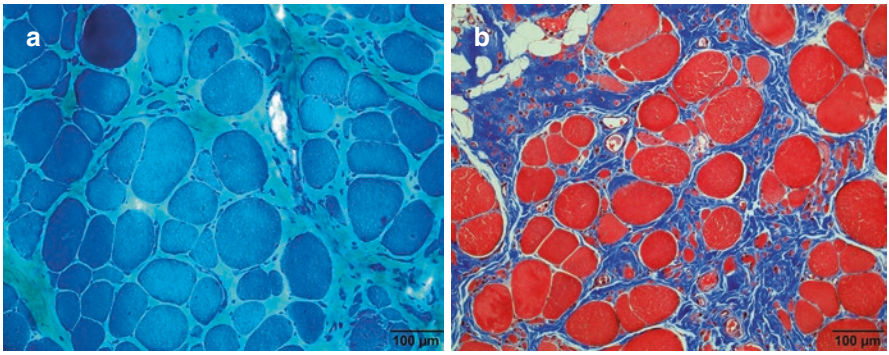

Fig. 1.21 Interstitial fibrosis. (**a**) Duchenne muscular dystrophy, Gomori trichrome. Increased endomysial connective tissue is a feature of many chronic myopathic disorders, including most muscular dystrophies. The abundant endomysial collagen in this biopsy stains light green in a cryostat section stained with the Gomori trichrome stain. (**b**) Duchenne muscular dystrophy, Masson trichrome. The endomysial collagen in a paraffin section from the same patient is highlighted dark blue in the Masson trichrome stain, contrasting sharply with the red color that the stain gives to the sarcoplasm of adjacent myofibers

confusion with the disrupted myosin and/or actin filaments that are often seen in injured myofibers. ***Non-lysosomal vacuoles*** are a feature of some of the non-lysosomal glycogen storage diseases, as well as some forms of periodic paralysis. Properly performed PAS stains reliably highlight the glycogen in vacuoles associated with glycogen storage diseases, while those associated with periodic paralysis are devoid of glycogen.

Changes in Connective Tissue

Endomysial fibrosis is commonly seen in chronic neuromuscular disorders (Fig. 1.21). Changes of this type are particularly common in chronic myopathic conditions, but can also be seen in severe, long-standing denervation. As muscle injury progresses, the areas previously occupied by skeletal muscle fibers are sometimes replaced by adipose tissue. In some biopsies, these connective tissue changes are so extensive that it is impossible to determine the nature of the underlying neuromuscular disease, and the biopsy must be designated simply as “end-stage muscle”.

Cellular Infiltrates

Inflammatory infiltrates are a common change in muscle biopsies, particularly in patients with myopathic disorders. The most common inflammatory cells are lymphocytes and macrophages (histiocytes), although other cell types – plasma cells, neutrophils and eosinophils – are sometimes encountered. ***Infiltrating lymphocytes*** are particularly important to recognize in muscle biopsies. Lymphocytic infiltrates can be encountered in any of the muscle compartments – endomysium, perimysium and even in epimysial connective tissue – and their distribution can provide important clues to the nature of the muscle disease. Endomysial lymphoid infiltrates are a feature of polymyositis (Fig. 1.22a), classically associated with lymphocytic invasion of non-necrotic myofibers by CD8-reactive T-lymphocytes. Identical patterns of endomysial inflammation are also seen in inclusion body myositis and in polymyositis with mitochondrial abnormalities. Perimysial lymphocytic infiltration (Fig. 1.22b), in contrast, is often seen in dermatomyositis and related inflammatory myopathic disorders, such as systemic lupus erythematosus-associated myositis, as well as in cases of primary inflammation of fascial connective tissue (fasciitis). While the presence of lymphocytic infiltration can be an important clue to the presence of an inflammatory myopathy responsive to immunomodulatory therapy, it is important to note that they can also be seen in myopathic processes that do not respond to immunosuppression, including inclusion body myositis, some muscular dystrophies (notably facioscapulohumeral dystrophy, dysferlin deficiency, merosin-deficient congenital muscular dystrophy and occasional dystrophinopathy cases). Conversely, lymphocytic infiltrates are not always present in biopsies from patients with immune-mediated myopathic disorders (e.g. immune-mediated necrotizing myopathies), and may be absent even in biopsies from patients with conventional inflammatory myopathies (e.g., polymyositis) due to "sampling error". ***Macrophages*** are almost invariably present in conditions associated with muscle fiber necrosis, where they engulf necrotic fibers, as illustrated earlier in Fig. 1.13b, and sometimes infiltrate the connective tissue adjacent to damaged myofibers. In such conditions, macrophages are a nonspecific host reaction to muscle fiber injury, and, as noted earlier, should not be misinterpreted as evidence of a primary inflammatory myopathic process. Less commonly, macrophages can be a component of a primary inflammatory process, exemplified by cases of macrophagic myofasciitis (Fig. 1.22c) an inflammatory muscle disease caused by the intramuscular injection of vaccines containing aluminum adjuvant [27], and in cases of granulomatous myositis.

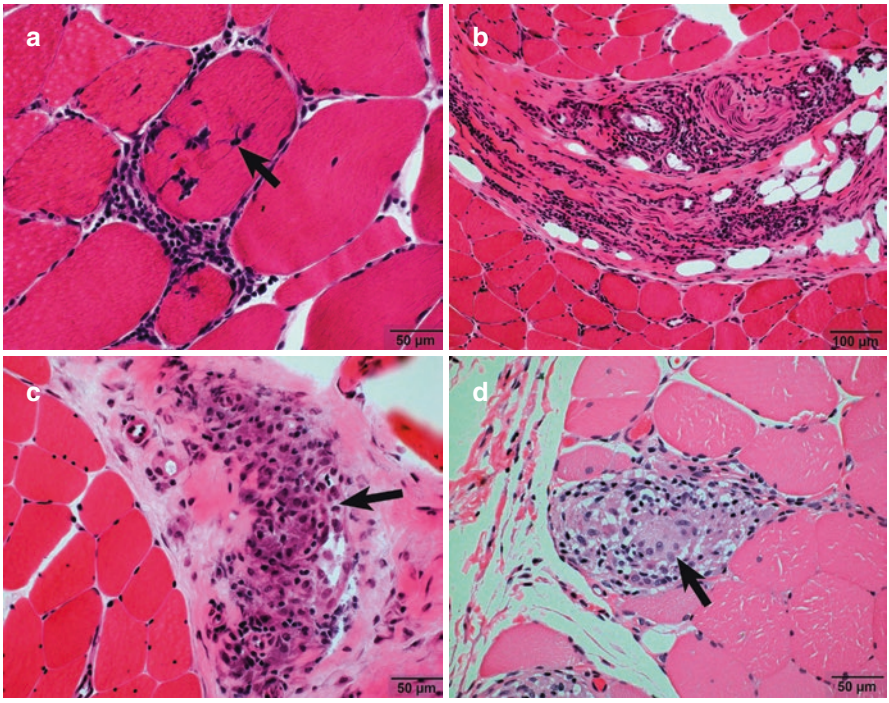

Fig. 1.22 Inflammatory infiltrates. (**a**) Endomysial inflammation with lymphocytic myofiber invasion in polymyositis, H&E. Lymphocytic infiltration of the endomysium is a feature of polymyositis and inclusion body myositis, and can also be seen in some forms of muscular dystrophy. Invasion of adjacent myofibers by lymphocytes (arrow) is seen in polymyositis and inclusion body myositis, but not in muscular dystrophies. (**b**)**,** Perimysial inflammation, H&E. Lymphocytic infiltration of the perimysial is common in dermatomyositis and related inflammatory myopathies, and is also a feature of some cases of fasciitis. (**c**) Macrophagic myofasciitis, H&E. Macrophages (arrow) are most often encountered in skeletal muscle as a host response to muscle fiber injury, but in some inflammatory conditions, including macrophagic myofasciitis, are the primary inflammatory cell. The cytoplasm of the macrophages in macrophagic myofasciitis has a characteristic granular, basophilic appearance. (**d**) Granulomatous inflammation, H&E. Granulomas are compact aggregates of activated macrophages, often associated with multinucleate giant cells (arrow). Granulomatous inflammation in skeletal muscle is a feature of sarcoidosis and a number of other non-infectious entities, but its presence should always prompt a search for microorganisms, particularly acid fast bacilli or fungi

Macrophagic infiltration associated with ***granulomatous inflammation*** can be seen in the muscles of patients with sarcoidosis (Fig. 1.22d), and, less commonly, in patients with thymoma, Crohn's disease, and isolated granulomatous myositis [62, 63]. Granulomatous inflammation can also be encountered in patients with inflammatory myopathy associated with the presence of anti-mitochondrial antibodies [64] and in some vasculitic disorders (discussed below). Finally, the possibility of an infectious process should always be excluded in patients with evidence of

granulomatous inflammation. Enzyme histochemical staining for acid phosphatase reactivity and immunohistochemical staining for CD68 reliably highlight the macrophagic infiltrates in cases of granulomatous myositis and other conditions. ***Plasma cells*** are less commonly encountered in muscle biopsies than either macrophages or lymphocytes. They may be conspicuous in cases of myositis associated with Sjogren's syndrome. ***Eosinophils*** can be seen in small numbers in inflammatory myopathies of various types, but are not usually conspicuous. Well-developed eosinophilic infiltrates have been reported in as an idiopathic focal lesion ("focal eosinophilic myositis"), as a manifestation of parasitic infection and in rare examples of muscle involvement in systemic hypereosinophilic syndrome [65] and in allergic granulomatosis [66]. They have also been reported in limb girdle muscular dystrophies associated with calpain-3 mutations [67] and γ-sarcoglycan mutations [68]. ***Neutrophilic infiltrates*** are also fairly uncommon in muscle biopsies. Their presence should prompt careful search for a bacterial or fungal infection. Sterile neutrophilic myositis has been reported in Sweet's syndrome [69] associated with hematologic malignancies and myelodysplastic disorders.

Vascular Changes

A variety of important diagnostic changes can be seen in the blood vessels in skeletal muscle biopsies. ***Amyloid deposits***, discussed earlier, are often associated with vessel walls in patients with amyloid myopathies. ***Thickening of vascular basal laminae*** is common in aging, hypertension and diabetes mellitus, and is also a conspicuous change in patients with an uncommon immune-mediated disorder designated necrotizing myopathy with pipestem capillaries [70]. Thickened basal laminae have a homogeneous, lightly eosinophilic appearance in H&E stains, appear pale green in Gomori trichrome-stained cryostat sections, and are highlighted in PAS stains. Thickened basal laminae are easily identified at an ultrastructural level (Fig. 1.23a), where it is often split and reduplicated. ***Dermatomyositis*** is associated with areas of reduced capillary density, deposition of terminal complement complex ($C_{5b\text{-}9}$) in perifascicular capillaries and, at an ultrastructural level, the presence of characteristic ***tubuloreticular inclusions*** in the cytoplasm of endothelial cells (Fig. 1.23b). For completeness, it should be noted that, while capillary C5b-9 deposition is a feature of a dermatomyositis and some additional immune-mediated myopathic processes, it is also commonly seen in endomysial capillaries in patients with diabetes mellitus in the absence of immune-mediated muscle injury [71]. ***Vasculitis*** can be seen in skeletal muscle in patients with a number systemic disorders, including polyarteritis nodosa, allergic granulomatosis (Churg-Strauss disease), rheumatoid arthritis, systemic lupus erythematosus and related connective tissue disorders. A spectrum of morphological patterns can be seen in cases of vasculitis, ranging from simple lymphocytic infiltration of vessel walls to fibrinoid necrosis and leukocytoclastic change (Fig. 1.23c). Vasculitis associated with

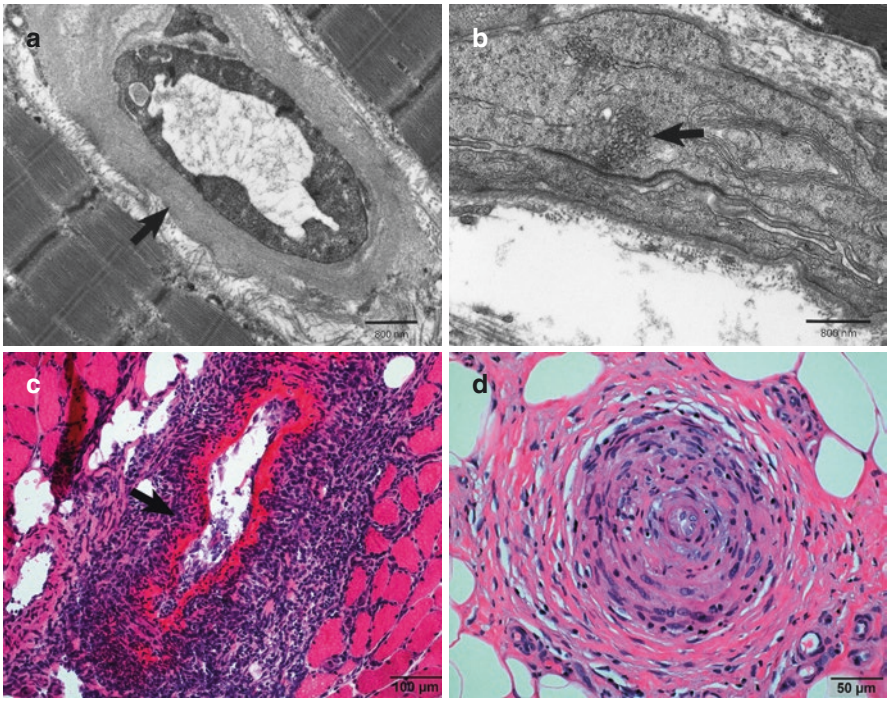

Fig. 1.23 Vascular changes. (**a**) Microvascular sclerosis, EM. Thickening of vascular basal laminae (arrow) can occur as a consequence of aging, but can also be an indicator of diabetes mellitus or hypertension. Basal lamina thickening has also been described in a variant of inflammatory myopathy known as necrotizing myopathy with pipestem capillaries. PAS stains are a useful technique for demonstrating basal lamina thickening at the light microscopic level. (**b**) Endothelial tubuloreticular inclusions in dermatomyositis, H&E. Tubuloreticular inclusions (arrow) in the cytoplasm of endothelial cells are a classical feature of dermatomyositis and related disorders such as lupus-associated myositis. (**c**) Necrotizing vasculitis, H&E. Necrotizing vasculitis is characterized by the presence of vessel wall inflammation associated with fibrinoid necrosis (arrow), the latter a brightly eosinophilic staining pattern caused by altered plasma proteins that have leaked into the wall of the injured vessel. (**d**) Remote vasculitic injury, H&E. When a vessel has been injured by vasculitis, cellular elements in the vessel wall proliferate in an attempt to repair the damage. The end result is often a markedly thickened, fibrotic vessel wall with an abnormally small lumen

granulomatous inflammation can be seen in patients with Wegener's granulomatosis and allergic granulomatosis. It is important to remember that vasculitis is a multifocal, rather than a diffuse, process, and that diagnostic changes may not be present in a single biopsy from a patient with a systemic vasculitic process. In such cases, serial sections of the specimen may disclose areas of vasculitis not represented in the initial sections. Search for evidence of remote vascular damage (e.g. asymmetrical fibrosis of the vessel wall, disruption of the elastic lamella or remote occlusion of the vessel lumen) may also provide clues to the presence of vasculitis (Fig. 1.23d). In the final analysis, a "negative" biopsy should never be taken as proof that that the possibility of vasculitis has been excluded.

Artifacts in Skeletal Muscle Biopsies

As noted in the comments on the proper acquisition of muscle biopsies, improper handling of muscle tissue at the time of biopsy, during transport to the laboratory or during processing in the laboratory can produce a range of artifacts ranging from alterations that are annoying but otherwise inconsequential to changes that preclude meaningful interpretation of the biopsy. An unfortunate and avoidable artifact commonly introduced at the time of biopsy is ***cautery artifact***. The cauterized muscle fibers have a condensed, dark appearance in H&E and trichrome stains (Fig. 1.24a) and are, predictably, devoid of normal enzyme activity. ***Formalin artifact***, cause by accidental exposure of fresh tissue destined for frozen section histology is another abnormality encountered in muscle tissue, particularly those submitted from institutions with less experience in performing neuromuscular biopsies. The affected myofibers in such cases stain diffusely red in the Gomori trichrome stain rather than green (Fig. 1.24b). There is typically a significant loss of enzyme activity in such cases, even after very brief, inadvertent exposure to formalin. An ***artifactual loss of enzyme activity*** can be seen in muscle tissue that has been transported in excess saline, or in which processing in the laboratory has been delayed. Some stains, including those for glycolytic pathway enzymes, are particularly sensitive to delayed processing, and "negative" reactions in such cases should be interpreted with caution. Prolonged immersion of fresh muscle into excess saline also tends to leach glycogen from the sarcoplasm**.** Mitochondrial enzymes, particularly cytochrome c oxidase, are also susceptible to artifactual degradation, which typically appears as a loss of enzyme activity at the edges

of the tissue (Fig. 1.24c). ***Ice crystal artifact*** is a common change in specimens that have been transported in excess saline. Ice crystal artifact is characterized by the presence of optically clear sarcoplasmic vacuoles of variable size and distribution (Fig. 1.24d), and can be confused with vacuoles associated with some vacuolar myopathies. Thawing and properly refreezing the tissue can sometimes reduce the amount of ice crystal artifact, although myofibers tend to shrink during this process. ***Drying artifact*** can occur if the fresh muscle segment is exposed to air for an excessive amount of time prior to freezing (Fig. 1.24e). Muscle fibers that have dried out tend to be rounded and retracted from the adjacent endomysium, and often have a pale, "smudgy" appearance in H&E stains. They usually stain poorly in enzyme histochemical preparations. Artifactual pallor is also commonly seen if fresh muscle has been immersed in

Fig. 1.24 Artifacts in skeletal muscle biopsies. (**a**) Cautery artifact, H&E. The use of an electrocautery instrument during excision of muscle tissue effectively "cooks" the myofibers, giving them a shrunken, dark, contracted appearance (arrow). This change precludes meaningful interpretation of the morphology of the affected tissue. (**b**) Formalin artifact, Gomori trichrome. Accidental immersion of fresh muscle into formalin causes the myofibers to stain red (arrow). These myofibers are effectively "fixed", and cannot be evaluated for the presence of enzyme activity or subtle changes in the intermyofibrillar network. (**c**) Artifactual loss of mitochondrial enzyme activity, sequential COX-SDH stain. Cytochrome c oxidase activity is often lost in muscles that have been subjected to drying or inadequate freezing during transport to the laboratory from remote locations. The artifactual loss of enzyme activity is most apparent at the edges of the tissue fragments (arrow). This pattern needs to be distinguished from the selective perifascicular loss of COX reactivity that can be seen in dermatomyositis. (**d**) Freezing artifact, H&E. Skeletal muscle that has been improperly frozen, or inadvertently thawed during transfer to the cryostat, contains irregular, optically clear vacuoles caused by the presence of ice crystals (arrows). These artifactual changes can be confused with true vacuolar change, and make evaluation of other morphological changes extremely difficult. (**e**) Drying artifact, H&E. Tissue that has been dried, as often happens when muscle is transported from a distant site, thawed and refrozen yields sections in which the muscle fibers are artifactually separated and stain poorly, particularly in enzyme histochemical preparations. If cryostat sections are allowed to air dry at room temperature for too long a time, they have a "smudgy", pale appearance in most stains. Abnormal sarcoplasmic pallor is also a feature of fresh muscle that has been immersed in excess saline prior to freezing. (**f**) Contraction artifact, EM. Immersion of fresh muscle tissue into aldehyde-based fixatives causes the muscle fiber to vigorously contract. This results in aggregation of normal contractile elements into amorphous, densely staining areas (arrow) that can obscure diagnostically significant changes in sarcomeric morphology, such as multiminicores. Contraction artifact can be minimized by clamping muscle segments *in situ* before excising them and placing them into fixative

excess saline during transport to the laboratory. ***Contraction artifact*** can occur when muscle segments are placed into fixative for subsequent paraffin or resin embedding. In some instances, this results in only occasional dense, hypercontracted segments in longitudinally oriented myofibers, but in more extreme cases, can completely obscure sarcomeric morphology and hamper the evaluation of the muscle biopsy for multi-minicores or other pathological patterns of sarcomeric disorganization (Fig. 1.24f). Contraction artifact can be minimized by clamping the muscle segment *in situ* prior to excising it and placing it into fixative.

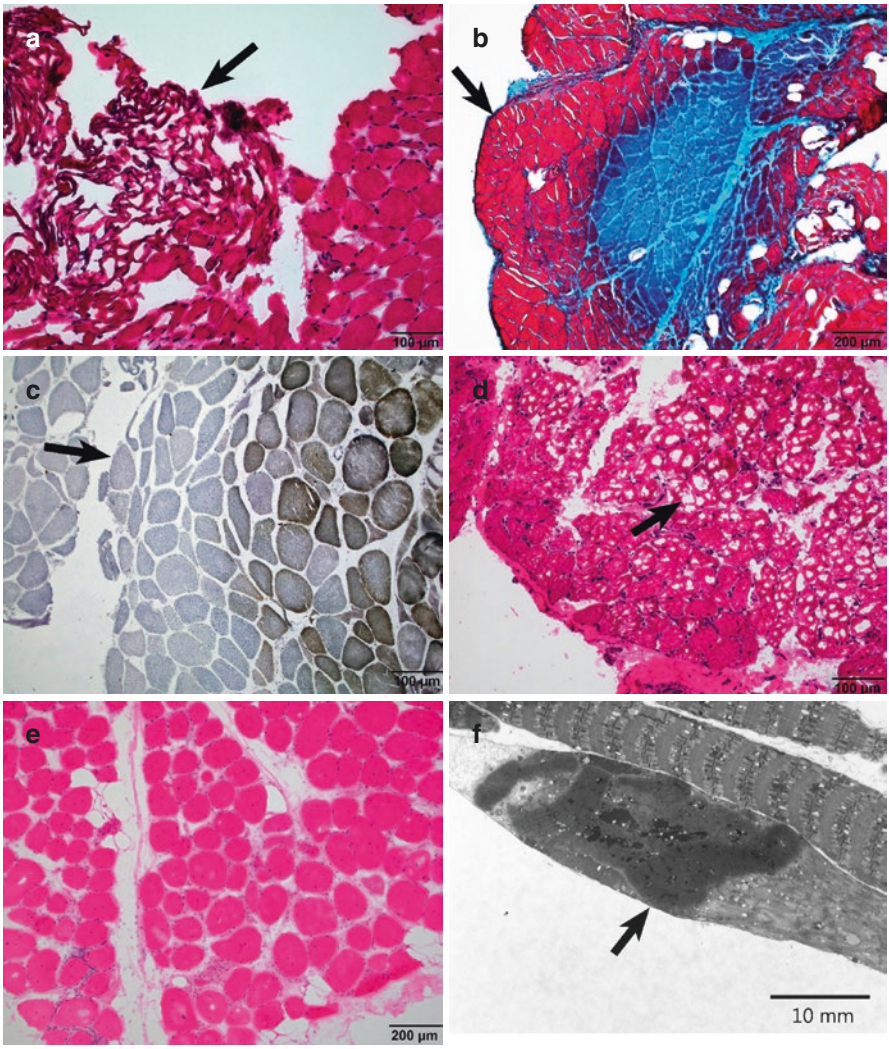

Acknowledgement The author gratefully acknowledges the many helpful suggestions from Drs. Lan Zhou and Chunyu Cai during the preparation of this chapter, and for special assistance provided by Dr. Zhou in the preparation of the section on muscle biopsy technique.

References

1. Dubowitz VS, Sewry CA, Oldfors A. Muscle biopsy a practical approach. Philadelphia. Sanders Elsevier: 4th ed; 2013.
2. Nance JR, Mammen AL. Diagnostic evaluation of rhabdomyolysis. Muscle Nerve. 2015;51(6):793–810.
3. Schiaffino S, Reggiani C. Fiber types in mammalian skeletal muscles. Physiol Rev. 2011;91(4):1447–531.
4. Staron RS, Hagerman FC, Hikida RS, Murray TF, Hostler DP, Crill MT, et al. Fiber type composition of the vastus lateralis muscle of young men and women. J Histochem Cytochem. 2000;48(5):623–9.
5. Engel WK. Focal myopathic changes produced by electromyographic and hypodermic needles. "Needle myopathy". Arch Neurol. 1967;16(5):509–11.
6. Edwards RH. Percutaneous needle-biopsy of skeletal muscle in diagnosis and research. Lancet. 1971;2(7724):593–5.
7. Edwards RH, Lewis PD, Maunder C, Pearse AG. Percutaneous needle biopsy in the diagnosis of muscle diseases. Lancet. 1973;2(7837):1070–1.
8. Edwards RH, Round JM, Jones DA. Needle biopsy of skeletal muscle: a review of 10 years experience. Muscle Nerve. 1983;6(9):676–83.
9. Engel WK, Cunningham GC. Rapid examination of muscle tissue. An improved trichrome method for fresh-frozen biopsy specimens. Neurology. 1963;13(11):919–23.
10. Round JM, Matthews Y, Jones DA. A quick, simple and reliable histochemical method for ATPase in human muscle preparations. Histochem J. 1980;12:707–10.
11. Sarnat HB. Muscle pathology and histochemistry. Chicago: American Society of Clinical Pathologists Press; 1983.
12. Barka T, Anderson PJ. Histochemistry theory and practice and bibliography. New York: Hoeber; 1963.
13. Engel KW, Cunningham GC. Alkaline phosphatase-positive abnormal muscle fibers of humans. J Histochem Cytochem. 1970;18:55–7.
14. De Paepe B, De Bleecker JL, Van Coster R. Histochemical methods for the diagnosis of mitochondrial diseases. Curr Protoc Hum Genet. 2009;19(2):1–19.
15. Ross JM. Visualization of mitochondrial respiratory function using cytochrome c oxidase/ succinate dehydrogenase double-labeling histochemistry. J Vis Exp. 2011;e3266:1–6.
16. Takeuchi T, Kuriaki H. Histochemical detection of phosphorylase in animal tissues. J Histochem Cytochem. 1955;3:153–60.
17. Bonilla E, Schotland DL. Histochemical diagnosis of muscle phosphofructokinase deficiency. Arch Neurol. 1970;8222:8–12.
18. Fishbein WN, Griffin JL, Armbrustmacher VW. Stain for skeletal muscle adenylate deaminase. An effective tetrazolium stain for frozen biopsy specimens. Arch Pathol Lab Med. 1980;104:463–6.
19. Brook MH, Engel WK. The histographic analysis of human muscle biopsies with respect to fiber types. 1. Adult male and female. Neurology. 1969;19(3):221–33.
20. Spuler S, Carl M, Zabojszcza J, Straub V, et al. Dysferlin-deficient muscular dystrophy features amyloidosis. Ann Neurol. 2008;63(3):323–8.
21. Milone M, Liewluck T, Winder TL, Pianosi PT. Amyloidosis and exercise intolerance in ANO5 muscular dystrophy. Neuromuscul Disord. 2012;22(1):13–5.
22. Clement CG, Truong LD. An evaluation of Congo red fluorescence for the diagnosis of amyloidosis. Hum Pathol. 2014;45:1766–72.
23. Chariot P, Ruet E, Authier FJ, Labes D, Poron F, Gherardi R. Cytochrome c oxidase deficiencies in the muscle of patients with inflammatory myopathies. Acta Neuropathol. 1996;91:530–6.
24. Alhatou M, Sladky JT, Bagasra O, Glass JD. Mitochondrial abnormalities in dermatomyositis: characteristic pattern of neuropathology. J Mol Histol. 2004;35:615–9.

25. Fishbein WN, Muldoon SM, Deuster PA, Armbrustmacher VW. Myoadenylate deaminase deficiency and malignant hyperthermia susceptibility: is there a realtionship? Biochem Med. 1985;34:344–54.
26. Fricker R, Bittner R, Böhm D, Shorney S, Gilly H, Kress HG. Malignant hyperthermia (MH) susceptibility and myoadenylate deaminase (MAD) deficiency. Eur J Anesth. 1997;14:82.
27. Chkheidze R, Burns DK, White CL 3rd, Castro D, Fuller J, Cai C. Morin stain detects aluminum-containing macrophages in macrophagic myofasciitis and vaccination granuloma with high sensitivity and specificity. J Neuropathol Exp Neurol. 2017;76:323–31.
28. Vogel H, Zamecnik J. Diagnostic immunohistology of muscle diseases. J Neuropathol Exp Neurol. 2005;64:181–93.
29. Tews DS, Goebel HH. Diagnostic immunohistochemistry in neuromuscular disorders. Histopathology. 2005;46:1–23.
30. Suriyonplengsaeng C, Dejthevaporn C, Khongkhatithum C, Sanpapant S, Tubthong N, Pindradap N, Srinark N, Waisayarat J. Immunohistochemistry of sarcolemmal membrane-associated proteins in formalin-fixed and paraffin-embedded skeletal muscle tissue: a promising tool for the diagnostic evaluation of comon muscular dystrophies. Diagn Pathol. 2017;12:19.
31. Bozzola JJ, Russell LD. Electron microscopy: principles and techniques for biologists. 2nd ed. Boston: Jones and Bartlett; 1992.
32. Romero NB. Centronuclear myopathies: a widening concept. Neuromuscul Disord. 2010;20:223–8.
33. Wilmshurst JM, Lillis S, Zhou H, Pillay K, Henderson H, Kress W, et al. RYR1 mutations are a common cause of congenital myopathies with central nuclei. Ann Neurol. 2010;68:717–26.
34. Sewry CA, Quinlivan RCM, Squier W, Morris GE, Holt I. A rapid immunohistochemical test to distinguish congenital myotonic dystrophy from X-linked myotubular myopathy. Neuromuscul Disord. 2012;22:225–30.
35. Lotz BP, Engel AG, Nishino H, Stevens JC, Litchy WJ. Inclusion body myositis. Observations in 40 patients. Brain. 1989;112:727–47.
36. Coquet M, Vital C, Julien J. Presence of inclusion body myositis-like filaments in oculopharyngeal muscular dystrophy. Ultrastructural study of 10 cases. Neuropathol Appl Neurobiol. 1990;16:393–400.
37. Stenzel W, Preuβe C, Allenbach Y, Pehl D, Junckerstorff R, Heppner FL, et al. Nuclear actin aggregatino is a hallmakr of anti-synthetase syndrome-induced dysimmune myopathy. Neurology. 2015;84:1346–54.
38. Koy A, Ilkovski B, Laing N, North K, Weis J, Mayatepek E, et al. Nemaline myopathy with exclusively intranuclear rods and a nobel mutation in ACTA1 (Q139H). Neuropediatrics. 2007;38:282–6.
39. Wu S, Ibarra MC, Malicdan MC, Murayama K, Ichihara Y, Nonaka I, et al. Central core disease is due to RYR1 mutations in more than 90% of patients. Brain. 2006;129:1470–80.
40. Ferreiro A, Monnier N, Romero NB, Leroy J-P, Bönneman C, Haenggeli C-A, Straub V, et al. A recessive form of central core disease, transiently presenting as multi-minicore disease, is associated with a homozygous mutation in the ryanodine receptor type 1 gene. Ann Neurol. 2002;51:750–9.
41. Figarella-Branger D, El-Dassouki M, Saenz A, Cobo AM, Malzac P, Tong S, et al. Myopathy with lobulated fibers: evidence for heterogeneous etiology and clincial presentation. Neuromuscul Dis. 2002;12:4–12.
42. Tsuburaya R, Suzuki T, Saiki K, Nonaka I, Sugito H, Hayashi YK, et al. Lobulated fibers in a patient with a 46-year history of limb-girdle muscle weakness. Neuropathology. 2011;31:455–7.
43. Weller B, Carpenter S, Lochmuller H, Karpati G. Myopathy with trabecular muscle fibers. Neuromuscul Dis. 1999;9:208–14.
44. Hilton-Jones D, Miller A, Parton M, Holton J, Sewry C, Hanna MG. Inclusion body myositis. Neuromuscul Dis. 2010;20:142–7.
45. Blume G, Pestronk A, Frank B, Johns DR. Polymyositis with cytochrome oxidase negative muscle fibres. Early quadriceps weakness and poor response to immunosuppressive therapy. Brain. 1997;120:39–45.
46. Wharton SB, Chan KK, Pickard JD, Anderson JR. Pearavertebral muscles in disease of the cervical spine. J Neurol Neurosurg Psychiatry. 1996;61:461–5.
47. Fayet G, Rouche A, Hogrel J-Y, Tomé FMS, Fardeau M. Age-related morphological changes in the deltoid muscle from 50 to 79 years of age. Acta Neuropathol. 2001;101:358–66.
48. Rosenberg NL, Neville HE, Ringel SP. Tubular aggregates. Their association with neuromuscular disease, including the syndrome of myalgias/cramps. Arch Neurol. 1985;42:973–6.

49. Romero NB, Sandaradura SA, Clarke NF. Recent advances in nemaline myopathy. Curr Opin Neurol. 2013;26:519–26.
50. Schröder JM, Sommer C, Schmidt B. Desmin and actin associated with cytoplasmic bodies in skeletal muscle fibers: immunohistochemical and fine structural studies, with a note on unusual 18- to 20-nm filaments. Acta Neuropathol. 1990;80:406–14.
51. Mateer JE, Farrell BJ, Chou SSM, Gutmann L. Reversible ipecac myopathy. Arch Neurol. 1985;42:188–90.
52. Foroud T, Pankratz N, Batchman AP, Pauciulo MW, Vidal R, Miravalle N, et al. A mutation in myotilin causes spheroid body myopathy. Neurology. 2005;65:1936–40.
53. Brooke MH, Neville HE. Reducing body myopathy. Neurology. 1972;22:829–40.
54. Schessl J, Taratuto AL, Sewry C, Battini R, Chin SS, Maiti B, et al. Clinical, histological and genetic characterization of reducing body myopathy caused by mutations in FHL1. Brain. 2009;132:452–64.
55. Nakano S, Engel AG, Wacklawik AJ, Emslie-Smith AM, Busis NA. Myofibrillar myopathy with abnormal foci of desmin positivity. I. Light and electron microscopy analysis of 10 cases. J Neuropathol Exp Neurol. 1996;55:549–62.
56. Olive M, Kley RA, Goldfarb MG. Myofibrillar myopathies: new developments. Curr Opin Neurol. 2013;26:527–35.
57. Askansas V, Engel WK, Nogalska A. Inclusion body myositis: a degenerative muscle disease associated with intra-muscle fiber multi-protein aggregates, proteasome inhibition, endoplasmic reticulum stress and decreased lysosomal degradation. Brain Pathol. 2009;19:493–506.
58. Broccolini A, Mirabella M. Hereditary inclusion body myopathies. Biochim Biophys Acta. 1852;2015:644–50.
59. Sugie K, Yamamoto A, Murayama K, Oh SJ, Takahashi M, Mora M, et al. Clinicopathological features of genetically confirmed Danon disease. Neurology. 2002;58:1773–8.
60. Kalimo H, Savontaus ML, Lang H, Paljarvi L, Sonninen V, Dean PB, et al. X-linked myopathy with excessive autophagy: a new hereditary muscle disease. Ann Neurol. 1988;23:258–65.
61. Ramachandran N, Munteanu I, Wang P, Ruggieri A, Rilstone JJ, Israelian N, et al. VMA21 deficiency prevents vacuolar ATPase assembly and causes autophagic vacuolar myopathy. Acta Neuropathol. 2013;25:439–57.
62. Le Roux K, Streichenberger N, Vial C, Petiot P, Feasson L, Bouhour F, et al. Granulomatous myositis: a clincial study of thirteen cases. Muscle Nerve. 2007;35:171–7.
63. Prieto-Gonzalez S, Grau JM. Diagnosis and classification of granulomatous myositis. Autoimmun Rev. 2014;13:372–4.
64. Maed MH, Tsuji S, Shimizu J. Inflammatory myopathies associated with anti-mitochondrial antibodies. Brain. 2012;135:1767–77.
65. Selva-O'Callaghan A, Trallero-Araguás E, Grau JM. Eosinophilic myositis: an updated review. Autoimmune Rev. 2014;13:375–8.
66. Vital A, Vital C, Viallard J-F, Ragnaud J-M, Canron MH, Lagueny A. Neuro-muscular biopsy in Churg-Strauss syndrome: 24 cases. J Neuropathol Exp Neurol. 2006;65:187–92.
67. Amato A. Adults with eosinophilic myositis and calpain-3 mutations. Neurology. 2008;70:730–1.
68. Baumeister SK, Todorovic S, Milać-Rašić V, Dekomien G, Lochmüller H, Walter MC. Eosinophilic myositis as presenting symptom in gamma-sarcoglycanopathy. Neuromuscul Disord. 2009;19:167–71.
69. Attias D, Laor R, Zuckermann E, Naschitz JE, Luria M, Misselevitch I, Boss JH. Acute neutrophilic myositis ins Sweet's syndrome: late phase transformation into fibrosing myositis and panniculitis. Hum Pathol. 1995;26:687–90.
70. Schröder NWJ, Goebel H-H, Brandis A, Ladhoff A-M, Heppner FL, Stenzel W. Pipestem capillaries in necrotizing myopathy revisited. Neuromuscul Disord. 2013;23:66–74.
71. Yell PC, Burns DK, Dittmar EG, White CL 3rd, Cai C. Diffuse microvascular C5b-9 deposition is a common feature in muscle and nerve biopsies from diabetic patients. Acta Neuropathol Commun. 2018;6(1):11.